

Distributed Downlink Precoding and Equalization in Satellite Swarms

Maik Röper, *Graduate Student Member, IEEE*, Bho Matthiesen, *Member, IEEE*,
Dirk Wübben, *Senior Member, IEEE*, Petar Popovski, *Fellow, IEEE*, and Armin
Dekorsy, *Senior Member, IEEE*

Abstract

In this paper, we propose a novel approach for downlink transmission from a satellite swarm towards a ground station (GS). These swarms have the benefit of much higher spatial separation in the transmit antennas than traditional satellites with antenna arrays, promising a massive increase in spectral efficiency. The resulting precoder and equalizer have very low demands on computational complexity, inter-satellite coordination and channel estimation. This is achieved by taking knowledge about the geometry between satellites and GS into account. For precoding, each satellite only requires its angles of departure (AoDs) towards the GS and it turns out that almost optimal rates can be achieved if the satellites transmit independent data streams. For the equalizer, the GS requires only knowledge about the angles of arrival (AoAs) from all satellites. Furthermore, we show that, by choosing a proper inter-satellite distance, the proposed low-complexity approach achieves the theoretical upper bound in terms of data rate. This optimal inter-satellite distance is obtained analytically under simplifying assumption and provides a heuristic for practical scenarios. Furthermore, a novel approach to increase the robustness of the proposed precoder and equalizer against imperfect AoD and AoA knowledge is proposed by exploiting the statistics of the estimation error.

This article was presented in part at 2022 IEEE Wireless Communications and Networking Conference [1].

M. Röper, B. Matthiesen, D. Wübben and A. Dekorsy are with the Gauss-Olbers Center, c/o University of Bremen, Dept. of Communications Engineering, 28359 Bremen, Germany (email: {roeper, matthiesen, wuebben, dekorsy}@ant.uni-bremen.de). P. Popovski is with Aalborg University, Department of Electronic Systems, 9220 Aalborg, Denmark (email: petarp@es.aau.dk). B. Matthiesen and P. Popovski are also with University of Bremen, U Bremen Excellence Chair, Dept. of Communications Engineering, 28359 Bremen, Germany.

This work is supported in part by the German Federal Ministry of Education and Research (BMBF) within the project Open6GHub under grant number 16KISK016 and by the German Research Foundation (DFG) under grant EXC 2077 (University Allowance).

Index Terms

Small-satellite swarms, MIMO, distributed precoding, angle division multiple access

I. INTRODUCTION

Integrating non-terrestrial networks (NTNs) into terrestrial communication systems is an important step towards truly ubiquitous connectivity [2], [3]. An essential building block are small satellites in low Earth orbit (LEO) that are currently deployed in private sector mega constellations [4]–[6]. Their main benefits are much lower propagation delays and deployment costs due to the LEO when compared to more traditional high-throughput satellites [7]–[9] in medium Earth orbit (MEO) and geostationary orbit (GEO). While current systems focus on connecting ground stations (GSs) to a single satellite, combining several low cost satellites in swarms leads to increased flexibility and scalability [10]. Satellite swarms are groups of small satellite flying quite close together and often acting as a single entity. In contrast to a constellation, their purpose is not to provide global coverage. A constellation might consists of several satellite swarms. The inter-satellite distances in satellite swarms range from less than a kilometer to several hundreds of kilometer [11], [12]. In this paper, an approach to determine an appropriate inter-satellite distance for high-throughput communication is presented. Indeed, the joint transmission of multiple satellites forming large virtual antenna arrays promises tremendous spectral efficiency gains solely due to the increased spatial separation of antennas [13], [14]. However, the straightforward implementation of the optimal precoder requires up-to-date channel state information (CSI) and timely inter-satellite coordination. This is infeasible due to very short channel coherence times resulting from high orbital velocities in combination with comparably large propagation delays, both in ground-to-satellite and in inter-satellite links.

In this paper, we consider a satellite swarm that jointly transmits towards a GS equipped with an antenna array, and develop a precoding approach that overcomes these obstacles by exploiting positional information about the satellites and the GS. In contrast to full CSI, this information is either available due to the inherent determinism of orbital mechanics or is estimated easily, even in frequency division duplex (FDD) systems, as it is based on geometric relations [15]–[17]. This leads to an approximate channel model inspired by [18], which is employed to derive a beamspace multiple-input-multiple-output (MIMO) [16], [19] based distributed linear precoder and equalizer. This precoder requires only, at each satellite, relative positional knowledge between itself and

the GS. It achieves close to optimal spectral efficiency, although it only requires modest inter-satellite coordination prior to transmission instead of time-critical (and, therefore, infeasible) live inter-satellite communication during downlink transmission. It also has very low computational complexity. We also extend the results to imperfect position knowledge and propose robust precoder and equalizer designs that exhibit considerable gain over heuristic solutions. Similarly, the equalizer only needs angle of arrival (AoA) information for the satellites and, given proper design of the satellite swarm, shows nearly optimal performance in terms of throughput.

In [13], the downlink (DL) from a satellite swarm with more than 50 nano-satellites towards a single antenna ground station (GS) is studied. It is shown that, if the signals of all satellites add up in phase at the GS, a high array gain is achieved. Communication between multiple satellites and a GS with multiple antennas is studied in [20], where an iterative interference cancellation algorithm is considered to deal with the large spatial correlation between two close GEO satellites. Furthermore, in [21] and [22], the capacity of multi-satellite systems is studied. In [23], a distributed precoding algorithm for a multi-user DL scenario that requires information exchange between the satellites is proposed based on the minimum mean-squared error (MMSE) criterion. In [14], a zero-forcing (ZF) equalizer at the ground terminal is proposed to simultaneously receive transmission from two satellites. The authors also numerically evaluate the impact of the inter-satellite distance with respect to (w.r.t.) the outage probability for the signal-to-interference-and-noise ratio (SINR). Instead, we analyze, among other things, the impact of the inter-satellite distance on the ergodic rate for an arbitrary number of satellites. We also derive the optimal inter-satellite distance analytically for special cases and show that it serves as a good heuristic in all other cases. In [17], [24], [25], beamspace MIMO is adapted for ground to satellite communications, focusing on scenarios involving a single satellite. In [17], a precoder for DL transmission and an equalizer for receiving in the uplink (UL) for a single satellite communicating with multiple devices on ground is proposed. By exploiting perfect knowledge about the geometric relations and the long term channel statistics, a similar rate could be achieved compared to the case with perfect CSI in the given scenario.

The design of robust precoders and equalizers that can improve the performance in presence of channel estimation errors is a well investigated subject for terrestrial scenarios [26]. The most common assumption is that the CSI is disturbed by an additive estimation error [27], [28]. In [29], [30], an extended error model for the precoder design is investigated by taking non-ideal hardware into account, resulting in an multiplicative error model. However, such error models are invalid

if the transceivers are designed based on the AoAs and angles of departure (AoDs). Instead, this leads to a multiplicative error model with high correlation among the different antennas. In [31], an equalizer is proposed to completely cancel interference from a broader range of possible AoAs. Another common heuristic approach is given by the so-called diagonal loading method, where a scaled identity matrix is added to the imperfectly estimated autocorrelation matrix in order to increase robustness [32]. Further heuristic robust equalizers are presented in [33], [34], where the diagonal loading approach is improved by taking the statistics of the estimation error into account. The approach most similar to our proposed robust equalizer is given in [35], where an unwanted jamming signal is suppressed while the desired signal may have its origin in a large geographical region. However, the scenario in [35] leads to different performance metrics and, hence, different equalization problems and approaches. Furthermore, in [31]–[35] only 2D scenarios are investigated, i.e., there exists only one AoA and AoD between each transmitter and receiver node. In this paper, we consider an extended 3D model with both, elevation and azimuth angle. In addition, we also consider arbitrarily distributed estimation errors with known probability density function (PDF), whereas only uniformly distributed errors are considered in [33]–[35]. This generalization complicates the analysis considerably and requires a different mathematical approach than in [33]–[35].

In this paper, the DL from a satellite swarm towards a GS is investigated. The focus is on the proper design of the distributed precoder and the corresponding equalizer, based on position knowledge, as well as the swarm layout. In particular, the main contributions are:

- A low complexity distributed precoder for satellite swarms is proposed, where the satellites transmit statistically independent data streams. Additionally, this precoder requires only local knowledge about the satellite's AoDs towards the GS. It is shown, that, with our approach, the capacity can be achieved under certain conditions and close to optimal data rates are achieved in most other cases.
- An optimal linear equalizer in terms of the achievable rate based on the GS's knowledge of the AoAs from the satellites and the second order channel statistics is derived.
- The inter-satellite distance which maximizes the achievable rate in a satellite swarm is obtained for a simplified scenario. It is numerically shown that the derived distance provides a good heuristic, for broader scenarios, such that the achievable rate is still close to the channel capacity with the proposed linear precoder and equalizer.
- A robust approach to reduce the performance degradation of our precoder and equalizer

due to imperfect AoD and AoA knowledge, respectively, is derived. This is achieved by taking statistical knowledge about the estimation error into account. This approach is not only novel in the context of satellite communications, but is also applicable to any scenario where the channel is determined by the AoD or AoA, e.g., in mmWave communication [16], [36] or radar [35].

The system model and fundamental results serving as benchmark are introduced in Section II. Then, in Section III, the proposed precoder and equalizer are developed under the assumption of perfect position knowledge. In Section IV, they are extended for imperfect position knowledge. The optimal distance between the satellites in a swarm is analyzed in Section V. This also gives further insight about the optimality of the proposed precoder. The proposed methods are evaluated numerically in Section VI and Section VII concludes the paper.

Notation: Column vectors are denoted by bold lowercase letters \mathbf{q} , while bold uppercase letters denote matrices \mathbf{Q} . Non-bold symbols denote scalar values q, Q . The j th element of a vector and (j, j') th elements of a matrix are denoted by $[\mathbf{q}]_j$ and $[\mathbf{Q}]_{j,j'}$, respectively. A set $\{\mathbf{Q}_1, \dots, \mathbf{Q}_J\}$ is denoted by $\{\mathbf{Q}_j\}_{j=1}^J$. Furthermore, $\text{diag}(q_1, \dots, q_N)$ denotes a diagonal matrix with elements q_1, \dots, q_N along its main diagonal. Correspondingly, block diagonal matrices are denoted by $\text{blkdiag}(\mathbf{Q}_1, \dots, \mathbf{Q}_N)$. The trace, transpose and conjugate transpose of a matrix \mathbf{Q} are denoted by $\text{tr}\{\mathbf{Q}\}$, \mathbf{Q}^T and \mathbf{Q}^H , respectively. Furthermore, $|q|$ and $|\mathbf{Q}|$ are the absolute value of the scalar q and determinant of matrix \mathbf{Q} , respectively. The ℓ_2 -norm of a vector \mathbf{q} is denoted as $\|\mathbf{q}\|_2$. Additionally, $\nabla_{\mathbf{Q}} f(\mathbf{Q}_0)$ denotes the derivative of the function f w.r.t. \mathbf{Q} and evaluated at \mathbf{Q}_0 . Finally, $\mathbb{E}_{\{\mathbf{Q}_j\}_{j=1}^J}\{\cdot\}$ denotes the expected value w.r.t. to the random variables $\mathbf{Q}_1, \dots, \mathbf{Q}_J$, \otimes the Kronecker product between two matrices, \mathbf{I}_N is the identity matrix of dimension $N \times N$ and $\mathbf{0}_{N \times N'}$ is the all zero matrix of dimension $N \times N'$.

II. SYSTEM MODEL AND PERFORMANCE BOUNDS

A. System Setup

Consider a swarm of N_S satellites which jointly communicate to a common GS. For each involved node, i.e., each of the N_S satellites and the GS, we can define a local coordinate reference system, as depicted in Fig. 1. The xy-plane of each local coordinate frame is aligned with the corresponding planar antenna array. Thus, the rotation of each node, i.e., satellite or GS, leads to a rotation of the corresponding local coordinate frame. Let d_ℓ be the distance between satellite ℓ and the GS, the position of that satellite in the GS-centered coordinate system, i.e., the

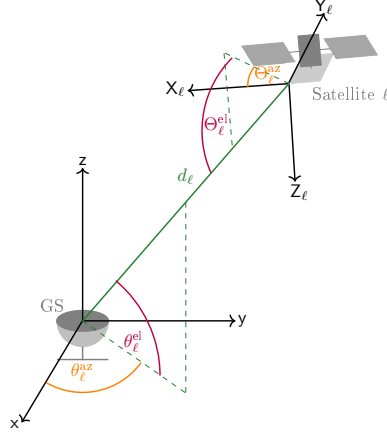


Fig. 1: Visualization of local coordinate frames.

relative position of the satellite w.r.t. the GS, is specified by the triplet $(d_\ell, \theta_\ell^{\text{el}}, \theta_\ell^{\text{az}})$, where θ_ℓ^{el} and θ_ℓ^{az} denote the elevation and azimuth angle in the GS-centered coordinate frame, respectively. Correspondingly, the position of the GS in the ℓ th satellite coordinate frame is given by the triplet $(d_\ell, \Theta_\ell^{\text{el}}, \Theta_\ell^{\text{az}})$, where Θ_ℓ^{el} and Θ_ℓ^{az} denote the elevation and azimuth angle in the ℓ th satellite coordinate frame, respectively. Given that the GS is located on a fixed position on the Earth and the satellites move on predefined orbits, the AoAs θ_ℓ^{el} and θ_ℓ^{az} can be extracted from the positions of satellite ℓ and the GS.

B. Generalized Communication Model

Satellite ℓ is equipped with an arbitrary planar antenna array consisting of N_t antennas and the GS uses an array with N_r antennas. The satellites jointly transmit a single common message known a priori at all satellites by encoding it in M independent data streams $\mathbf{s} \in \mathbb{C}^M$ using independent and identically distributed (i.i.d.) unit variance Gaussian codebooks. Partitioning the common message into data streams requires inter-satellite coordination prior to transmission. Satellite ℓ employs linear precoding, with its local precoding matrix $\mathbf{G}_\ell \in \mathbb{C}^{N_t \times M}$, to transmit the signal $\mathbf{x}_\ell = \mathbf{G}_\ell \mathbf{s} \in \mathbb{C}^{N_t}$. In a satellite swarm, all satellites are usually of the same type [10] and, thus, we assume that all satellites have the same average transmit power constraint ρ , i.e., $\text{tr} \{ \mathbf{G}_\ell \mathbf{G}_\ell^H \} \leq \rho$ for all $\ell = 1, \dots, N_S$. Furthermore, the signal received at the GS is

$$\mathbf{y} = \sum_{\ell=1}^{N_S} \mathbf{H}_\ell \mathbf{x}_\ell + \mathbf{n} \quad (1)$$

where \mathbf{n} is i.i.d. circularly-symmetric complex white Gaussian noise with power σ_n^2 and $\mathbf{H}_\ell \in \mathbb{C}^{N_r \times N_t}$ is the local channel matrix from satellite ℓ to the GS. Due to the collaborative transmission, this is effectively a point-to-point channel. In particular, let $\mathbf{H} = [\mathbf{H}_1, \dots, \mathbf{H}_{N_s}]$ be the composite channel matrix and $\mathbf{x} = [\mathbf{x}_1^T, \dots, \mathbf{x}_{N_s}^T]^T$ the composite transmit signal. Then, we can write (1) as $\mathbf{y} = \mathbf{H}\mathbf{x} + \mathbf{n}$.

Assuming joint precoding over all satellites, the channel capacity is upper bounded by [37]

$$R_{\text{opt}} = \max_{\text{tr}\{\mathbf{G}\mathbf{G}^H\} \leq N_s \rho} \log_2 \left| \mathbf{I}_{N_r} + \frac{1}{\sigma_n^2} \mathbf{H}\mathbf{G}\mathbf{G}^H\mathbf{H}^H \right|, \quad (2)$$

where $\mathbf{G} = [\mathbf{G}_1^T, \dots, \mathbf{G}_{N_s}^T]^T \in \mathbb{C}^{N_{\text{Tx}} \times M}$ is the joint precoding matrix with $N_{\text{Tx}} = N_s N_t$ transmit antennas in total. Furthermore, we assume $M = \text{rank}(\mathbf{H})$. The maximum in (2) is achieved for

$$\mathbf{G}_{\text{opt}} = \mathbf{V}\mathbf{P}^{\frac{1}{2}}, \quad (3)$$

where the columns of \mathbf{V} are the M right singular vectors of \mathbf{H} , corresponding to the $M \leq N_{\text{Tx}}$ non-zero singular values, and $\mathbf{P} = \text{diag}(p_1, \dots, p_M)$ is the optimal transmit power allocation obtained from the waterfilling algorithm such that $\sum_{\mu} p_{\mu} = N_s \rho$, with p_{μ} being the transmit power of the μ th stream [37]. Combining (2) and (3), we obtain

$$R_{\text{opt}} = \sum_{\mu=1}^M \log_2 \left(1 + \lambda_{\mu} \frac{p_{\mu}}{\sigma_n^2} \right), \quad (4)$$

where λ_{μ} is the μ th eigenvalue of $\mathbf{H}\mathbf{H}^H$ [37], [38]. Note that this singular value decomposition (SVD)-based precoder design incorporates several assumptions that renders it infeasible for satellite swarms. First of all, an accurate estimate of \mathbf{H} is required. Due to the fast ground speeds of LEO satellites, the channel coherence time is rather short. Combined with the long round trip times between satellites and GS, obtaining this estimate with conventional methods appears to be impossible. Further, assuming a timely and accurate estimate of \mathbf{H}_ℓ exists at satellite ℓ , this estimate would have to be shared with all other satellites within the swarm, leading to additional delay and, thus, ageing of the channel estimate. Finally, the bound in (2) has a relaxed sum power constraint over all satellites that might lead to the violation of the power constraints of individual satellites. However, while being of little practical relevance, it gives the theoretical upper bound for the achievable rate that can serve as benchmark. In the following, we design a precoder and an equalizer that require only knowledge of rather long-term fading statistics and positional knowledge of the satellites and the GS, together with synchronized clocks between satellites for coherent transmission.

III. GEOMETRY BASED DL TRANSMISSION

In this section, we exploit positional information about the satellites and the GS to estimate the dominant large-scale components of the channel matrix \mathbf{H} . This results in a geometrical channel model that is subsequently employed to design a distributed linear precoder together with a linear equalization scheme at the GS. This approach does not require any inter-satellite coordination beyond clock synchronization and is not subject to the limitations of conventional CSI acquisition resulting from the short channel coherence time and long transmission distances.

A. Geometrical Channel Approximation

Observe that the channels from the antennas of a single satellite to the GS are highly correlated [18] and, thus, there are only $M \leq N_S \leq N_{Tx}$ singular values larger than zero. Further, assume that the communication between satellites and the GS takes place under line-of-sight (LOS) conditions, which is a very typical scenario in satellite communications. Then, the channel matrix \mathbf{H} is exclusively determined by the distances between transmit and receive antennas as well as atmospheric effects [39], [40]. Moreover, due to the LOS connection and the large distance between satellites and GS, the channels of the antennas from satellite ℓ to the ground station are subject to approximately the same atmospheric effects [40]. Thus, it is reasonable to assume that the entries in \mathbf{H}_ℓ have equal magnitude and differ only in their phase.

Let $(D_{Rx,m}^x, D_{Rx,m}^y, 0)$ be the Cartesian coordinates of the m th antenna at the GS, given in the GS-centered coordinate frame, as depicted in Fig. 2 for an exemplary uniform rectangular array (URA). Then, due to the large distance between the satellites and the GS, the electromagnetic wave radiated by satellite ℓ arrives approximately as a plane wave [17], [39] and the phase rotation due to the transmission channel observed at the m th GS-antenna is approximately

$$\phi_m^\ell \approx \nu \left(D_{Rx,m}^x \cos(\theta_\ell^{\text{el}}) \cos(\theta_\ell^{\text{az}}) + D_{Rx,m}^y \cos(\theta_\ell^{\text{el}}) \sin(\theta_\ell^{\text{az}}) \right) + \phi_0^\ell \quad (5a)$$

$$= \nu \left(D_{Rx,m}^x \phi_\ell^x + D_{Rx,m}^y \phi_\ell^y \right) + \phi_0^\ell, \quad m = 1, \dots, N_r \quad (5b)$$

where $\phi_\ell^x = \cos(\theta_\ell^{\text{el}}) \cos(\theta_\ell^{\text{az}})$, $\phi_\ell^y = \cos(\theta_\ell^{\text{el}}) \sin(\theta_\ell^{\text{az}})$ are the space angles in x- and y-direction, respectively, ϕ_0^ℓ is a phase offset, which is the same for all receive antennas, and $\nu = 2\pi f_c / c_0$ is the wavenumber.

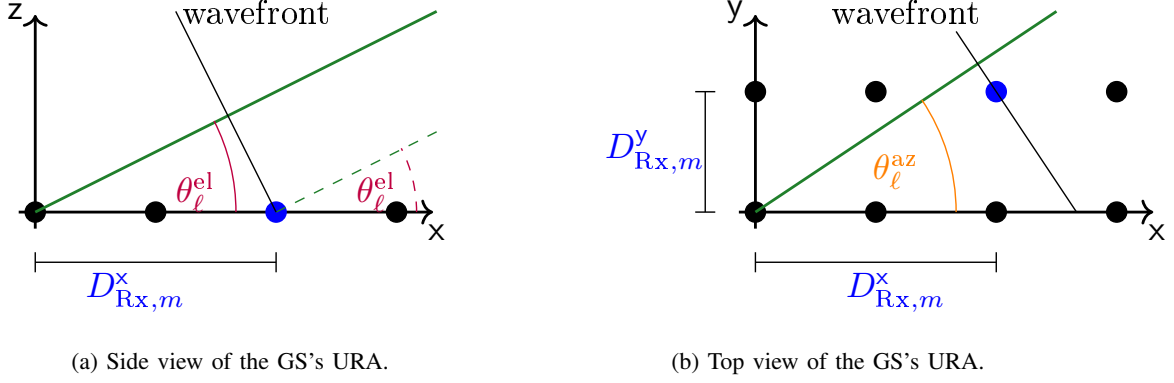


Fig. 2: Visualization of the AoAs for a wavefront arriving at the GS with a URA.

Likewise, let $(D_{Tx,n}^{x,\ell}, D_{Tx,n}^{y,\ell}, 0)$ be the Cartesian coordinates of the n th antenna of satellite ℓ , given in the ℓ th satellite-centered coordinate frame. Then, the signal, radiated by the n th antenna of satellite ℓ and arriving at the $m = 1$ st receive antenna at the GS, is rotated by

$$\Phi_n^\ell \approx \nu \left(D_{Tx,n}^{x,\ell} \cos(\Theta_\ell^{el}) \cos(\Theta_\ell^{az}) + D_{Tx,n}^{y,\ell} \cos(\Theta_\ell^{el}) \sin(\Theta_\ell^{az}) \right) + \Phi_0^\ell \quad (6a)$$

$$= \nu \left(D_{Tx,n}^{x,\ell} \Phi_\ell^x + D_{Tx,n}^{y,\ell} \Phi_\ell^y \right) + \Phi_0^\ell, \quad n = 1, \dots, N_t \quad (6b)$$

where $\Phi_\ell^x = \cos(\Theta_\ell^{el}) \cos(\Theta_\ell^{az})$, $\Phi_\ell^y = \cos(\Theta_\ell^{el}) \sin(\Theta_\ell^{az})$ are the space angles in x- and y-direction, respectively and Φ_0^ℓ is a phase offset, which is the same for all antennas at satellite ℓ . Note that the phase offsets $\phi_0^\ell \in [0, 2\pi]$ and $\Phi_0^\ell \in [0, 2\pi]$ include the distance d_ℓ as well as the atmospheric effects. Now, the approximated channel coefficient $\tilde{h}_{m,n}^\ell$ from the n th antenna at satellite ℓ to the m th receive antenna can be written as

$$\tilde{h}_{m,n}^\ell = \alpha_\ell e^{j\nu(D_{Rx,m}^x \phi_\ell^x + D_{Rx,m}^y \phi_\ell^y + D_{Tx,n}^{x,\ell} \Phi_\ell^x + D_{Tx,n}^{y,\ell} \Phi_\ell^y)} \quad (7)$$

where $\alpha_\ell = |\alpha_\ell| e^{j(\Phi_0^\ell + \phi_0^\ell)}$ is the i. i. d. complex-valued channel gain from satellite ℓ to the GS with $\mathbb{E}_{\alpha_\ell}\{\alpha_\ell\} = 0$ and $\mathbb{E}_{\alpha_\ell}\{|\alpha_\ell|^2\} = \sigma_{\alpha_\ell}^2$, which includes the free space path loss and the atmospheric effects. From these observations, we can define the steering vectors \mathbf{a}_ℓ and \mathbf{b}_ℓ . The vector \mathbf{a}_ℓ contains the phase differences at the receive antennas, while \mathbf{b}_ℓ contains the phase differences from the transmit antennas at satellite ℓ . Thus, their elements are

$$[\mathbf{a}_\ell]_m = a_{\ell,m} = e^{j\nu(D_{Rx,m}^x \phi_\ell^x + D_{Rx,m}^y \phi_\ell^y)}, \quad [\mathbf{b}_\ell]_n = b_{\ell,n} = e^{-j\nu(D_{Tx,n}^{x,\ell} \Phi_\ell^x + D_{Tx,n}^{y,\ell} \Phi_\ell^y)} \quad (8)$$

and the approximate channel matrix becomes

$$\tilde{\mathbf{H}}_\ell = \alpha_\ell \mathbf{a}_\ell \mathbf{b}_\ell^H \approx \mathbf{H}_\ell. \quad (9)$$

Further, we define $\mathbf{A} = [\mathbf{a}_1, \dots, \mathbf{a}_{N_S}]$. Observe that $\tilde{\mathbf{H}}_\ell$ has rank one if $\alpha_\ell \neq 0$, for all ℓ . Then, due to $N_r \geq N_S$ and the satellites having different positions in the orbital plane, i.e., $\theta_i \neq \theta_\ell$, for all $i \neq \ell$, the overall channel matrix $\tilde{\mathbf{H}} = [\alpha_1 \mathbf{a}_1 \mathbf{b}_1^H, \dots, \alpha_{N_S} \mathbf{a}_{N_S} \mathbf{b}_{N_S}^H]$ has rank N_S , which allows for the parallel transmission of $M = N_S$ independent streams. This, however, is only true for the approximated channel and does not necessarily hold for the real channel. Indeed, M can be less than N_S for a very small inter-satellite distance and this approach stops working. The choice of a proper inter-satellite distance will be discussed further in Section V.

This geometric approximation simplifies channel estimation and tracking considerably, mainly due to two reasons: First, the angles $\theta_\ell^{\text{cl}}, \theta_\ell^{\text{az}}, \Theta_\ell^{\text{cl}}, \Theta_\ell^{\text{az}}$ and, correspondingly, the space angles $\phi_\ell^x, \phi_\ell^y, \Phi_\ell^x, \Phi_\ell^y$ are independent of the carrier frequency and, thus, can be easily estimated in FDD systems [15]. Second, a priori knowledge about the positions and the deterministic satellite movement can be exploited to increase estimation accuracy. In the following, the precoder and equalizer are designed based on the steering vectors \mathbf{b}_ℓ and \mathbf{a}_ℓ (8), respectively.

B. Precoding

Given the geometric channel approximation $\tilde{\mathbf{H}}$, we design a precoder \mathbf{G}_{geo} that maximizes the average received power given the per-satellite power constraint, i.e., the solution to

$$\mathbf{G}_{\text{geo}} \in \arg \max_{\forall \ell: \text{tr}\{\mathbf{G}_\ell^H \mathbf{G}_\ell\} \leq \rho} \mathbb{E}_{\{\alpha_\ell\}_{\ell=1}^{N_S}} \left\{ \text{tr} \left\{ \mathbf{G}^H \tilde{\mathbf{H}}^H \tilde{\mathbf{H}} \mathbf{G} \right\} \right\}. \quad (10)$$

An optimal precoder with respect to (10) is stated in the following proposition.

Proposition 1. *A precoder that maximizes the received signal power under per-satellite power constraint, i.e., a solution to (10), is*

$$\mathbf{G}_{\text{geo}} = \sqrt{\frac{\rho}{N_t}} \text{blkdiag}(\mathbf{b}_1, \dots, \mathbf{b}_{N_S}) = \text{blkdiag}(\mathbf{g}_{1,\text{geo}}, \dots, \mathbf{g}_{N_S,\text{geo}}). \quad (11)$$

Proof: Define the matrices $\mathbf{B} = \text{blkdiag}(\mathbf{b}_1, \dots, \mathbf{b}_{N_S})$ and $\Sigma_\alpha = \text{diag}(\alpha_1, \dots, \alpha_{N_S})$. Then, the channel matrix $\tilde{\mathbf{H}}$ can be decomposed as $\tilde{\mathbf{H}} = \mathbf{A} \Sigma_\alpha \mathbf{B}^H$. Note that \mathbf{A} and \mathbf{B} are both deterministic. Thus, the objective function in (10) is equivalent to

$$\begin{aligned} & \mathbb{E}_{\{\alpha_\ell\}_{\ell=1}^{N_S}} \left\{ \text{tr} \left\{ \mathbf{G}^H \tilde{\mathbf{H}}^H \tilde{\mathbf{H}} \mathbf{G} \right\} \right\} \\ &= \mathbb{E} \left\{ \text{tr} \left\{ \mathbf{G}^H \mathbf{B} \Sigma_\alpha^H \mathbf{A}^H \mathbf{A} \Sigma_\alpha \mathbf{B}^H \mathbf{G} \right\} \right\} = \text{tr} \left\{ \mathbf{G}^H \mathbf{B} \mathbb{E} \left\{ \Sigma_\alpha^H \mathbf{A}^H \mathbf{A} \Sigma_\alpha \right\} \mathbf{B}^H \mathbf{G} \right\} \\ &= \text{tr} \left\{ \mathbf{G}^H \mathbf{B} N_r \mathbb{E} \left\{ \Sigma_\alpha^H \Sigma_\alpha \right\} \mathbf{B}^H \mathbf{G} \right\} = N_r \sum_{\ell=1}^{N_S} \sigma_{\alpha_\ell}^2 \text{tr} \left\{ \mathbf{G}_\ell^H \mathbf{b}_\ell \mathbf{b}_\ell^H \mathbf{G}_\ell \right\}. \end{aligned} \quad (12)$$

Since $\mathbf{b}_\ell \mathbf{b}_\ell^H$ is positive semi-definite and $\sigma_{\alpha_\ell}^2$ and N_r are positive constants, the objective function is maximized if each term in (12) is maximized separately. Hence, the optimization problem (10) is equivalent to

$$\min_{\mathbf{G}_\ell} -\text{tr} \{ \mathbf{G}_\ell^H \mathbf{b}_\ell \mathbf{b}_\ell^H \mathbf{G}_\ell \} \quad \text{s.t.} \quad \text{tr} \{ \mathbf{G}_\ell^H \mathbf{G}_\ell \} \leq \rho, \quad \ell = 1, \dots, N_S \quad (13)$$

and the corresponding Lagrangian function is

$$\mathcal{L}_{\text{pc}}(\mathbf{G}_\ell, \omega_\ell) = -\text{tr} \{ \mathbf{G}_\ell^H \mathbf{b}_\ell \mathbf{b}_\ell^H \mathbf{G}_\ell \} + \omega_\ell (\text{tr} \{ \mathbf{G}_\ell^H \mathbf{G}_\ell \} - \rho) \quad (14)$$

where $\omega_\ell \geq 0$ is the Lagrange multiplier corresponding to the ℓ th power constraint.

We leverage [41, Prop. 3.3.4] to find the solution of (13). Every stationary point \mathbf{G}'_ℓ satisfies $\nabla_{\mathbf{G}} \mathcal{L}_{\text{pc}}(\mathbf{G}'_\ell, \omega'_\ell) = -\mathbf{G}'_\ell{}^H \mathbf{b}_\ell \mathbf{b}_\ell^H + \omega'_\ell \mathbf{G}'_\ell{}^H = \mathbf{0}$, for some ω'_ℓ . This is equivalent to

$$\mathbf{b}_\ell \mathbf{b}_\ell^H \mathbf{G}'_\ell = \omega'_\ell \mathbf{G}'_\ell, \quad (15)$$

which holds either if $\mathbf{G}'_\ell = \mathbf{0}_{N_t \times N_S}$ or ω'_ℓ is an eigenvalue of $\mathbf{b}_\ell \mathbf{b}_\ell^H$. Since, $\mathbf{b}_\ell \mathbf{b}_\ell^H$ is of rank one, its only eigenvalue is given by [42, Thm. 1.2.12]

$$\omega'_\ell = \text{tr} \{ \mathbf{b}_\ell \mathbf{b}_\ell^H \} = \sum_{n=1}^{N_t} e^{j0} = N_t. \quad (16)$$

Consider $\mathbf{G}'_\ell = \mathbf{0}$. Then, $\mathcal{L}_{\text{pc}}(\mathbf{0}, \omega_\ell) = -\omega_\ell \rho$. Since $\text{tr} \{ \mathbf{G}'_\ell{}^H \mathbf{G}'_\ell \} < \rho$, $\omega_\ell^* = 0$ [41, Prop. 3.3.4]. Hence, the case $\mathbf{G}'_\ell = \mathbf{0}$ is irrelevant when considering $\omega'_\ell = N_t$.

Substitute (15) and (16) into (14). Then, at every stationary point with $\mathbf{G}'_\ell \neq \mathbf{0}$,

$$\mathcal{L}_{\text{pc}}(\mathbf{G}'_\ell, \omega'_\ell) = -N_t \text{tr} \{ \mathbf{G}'_\ell{}^H \mathbf{G}'_\ell \} + N_t (\text{tr} \{ \mathbf{G}'_\ell{}^H \mathbf{G}'_\ell \} - \rho) = -N_t \rho \quad (17)$$

which is the minimum value of $\mathcal{L}_{\text{pc}}(\mathbf{G}_\ell, \omega'_\ell)$. Since

$$\mathcal{L}_{\text{pc}}(\mathbf{G}_{\ell, \text{geo}}, \omega'_\ell) = -\text{tr} \left\{ \sqrt{\frac{\rho}{N_t}} \mathbf{b}_\ell^H \mathbf{b}_\ell \mathbf{b}_\ell^H \sqrt{\frac{\rho}{N_t}} \mathbf{b}_\ell \right\} + N_t \left(\text{tr} \left\{ \sqrt{\frac{\rho}{N_t}} \mathbf{b}_\ell^H \sqrt{\frac{\rho}{N_t}} \mathbf{b}_\ell \right\} - \rho \right) \quad (18)$$

$$= -\frac{\rho}{N_t} (\mathbf{b}_\ell^H \mathbf{b}_\ell) (\mathbf{b}_\ell^H \mathbf{b}_\ell) + \rho (\mathbf{b}_\ell^H \mathbf{b}_\ell) - N_t \rho = -N_t \rho \quad (19)$$

$\mathbf{G}_{\ell, \text{geo}}$ is a global minimizer of $\mathcal{L}_{\text{pc}}(\mathbf{G}_\ell, \omega'_\ell)$. Further, since

$$\text{tr} \{ \mathbf{G}_{\ell, \text{geo}}^H \mathbf{G}_{\ell, \text{geo}} \} = \text{tr} \left\{ \sqrt{\frac{\rho}{N_t}} \mathbf{b}_\ell^H \sqrt{\frac{\rho}{N_t}} \mathbf{b}_\ell \right\} = \rho \quad (20)$$

$\mathbf{G}_{\ell, \text{geo}}$ is a solution to (13) [41, Prop. 3.3.4]. ■

A direct consequence of the block diagonal precoding matrix \mathbf{G}_{geo} is that each satellite transmits a different independent stream s_ℓ of the whole data vector \mathbf{s} , i.e., the transmit signal of satellite ℓ is $\mathbf{x}_\ell = \mathbf{G}_{\ell, \text{geo}} \mathbf{s} = \mathbf{g}_{\ell, \text{geo}} s_\ell$. Furthermore, the precoding vector $\mathbf{g}_{\ell, \text{geo}}$ for satellite ℓ

is independent of the precoding vectors $\mathbf{g}_{i,\text{geo}}$ for the other satellites $i \neq \ell$. Instead, satellite ℓ only has to know its AoD Θ_ℓ . This means that, due to the geometric channel approximation, the optimal solution to (10) can be obtained if the data stream is split among the satellites and each satellite processes its precoding vector locally. This is remarkable in so far that cooperative DL transmission is enabled without the requirement for inter-satellite information exchange during the transmission. Additionally, no costly SVD is needed for this approach. Instead, the proposed precoding is based on manipulating only the phase at each antenna and, thus, an efficient implementation with a single RF chain per satellite is possible [16].

C. Linear Equalization

Employing the previously derived precoder \mathbf{G}_{geo} , the received signal at the GS is

$$\mathbf{y} = \mathbf{H}\mathbf{G}_{\text{geo}}\mathbf{s} + \mathbf{n} = \sum_{\ell=1}^{N_S} \mathbf{H}_\ell \mathbf{g}_{\ell,\text{geo}} s_\ell + \mathbf{n}. \quad (21)$$

Now, we consider linear reception at the GS to recover the N_S data streams. In particular, after linear equalization with $\mathbf{W} = [\mathbf{w}_1, \dots, \mathbf{w}_{N_S}]^H \in \mathbb{C}^{N_S \times N_r}$, the ℓ th estimated stream is

$$\hat{s}_\ell = \mathbf{w}_\ell^H \mathbf{y} = \mathbf{w}_\ell^H \mathbf{H}_\ell \mathbf{g}_{\ell,\text{geo}} s_\ell + \mathbf{w}_\ell^H \left(\sum_{i \neq \ell} \mathbf{H}_i \mathbf{g}_{i,\text{geo}} s_i + \mathbf{n} \right). \quad (22)$$

Assuming the use of capacity achieving point-to-point codes for all streams, the achievable rate R_{lin} is the sum over the maximum per-stream rates [38, §8.3], i.e.,

$$R_{\text{lin}} = \sum_{\ell=1}^{N_S} R_\ell = \sum_{\ell=1}^{N_S} \log_2 (1 + \Gamma_\ell) \quad (23)$$

where

$$\Gamma_\ell = \frac{|\mathbf{w}_\ell^H \mathbf{H}_\ell \mathbf{g}_{\ell,\text{geo}}|^2}{\sum_{i \neq \ell} |\mathbf{w}_\ell^H \mathbf{H}_i \mathbf{g}_{i,\text{geo}}|^2 + \sigma_n^2 \mathbf{w}_\ell^H \mathbf{w}_\ell} \quad (24)$$

is the effective SINR of the ℓ th stream. Observe that Γ_ℓ is not a function of \mathbf{w}_i for all $i \neq \ell$. Thus, the rate in (23) is maximized by maximizing each term separately. Due to the monotonicity of the logarithm, this optimum is obtained at the maximum Γ_ℓ . However, determining the optimal equalizers with respect to (24) would require full CSI knowledge at the GS, which is difficult to obtain [17]. Instead, we employ the geometrical approximation $\tilde{\mathbf{H}}$ of \mathbf{H} and derive an equalizer with respect to $\Gamma_\ell|_{\mathbf{H}=\tilde{\mathbf{H}}}$. Since $\tilde{\mathbf{H}}_\ell$ still depends on the unknown fading factor α_ℓ , we optimize the mean SINR instead of the instantaneous, i.e.,

$$\mathbf{w}_{\ell,\text{geo}} \in \arg \max_{\mathbf{w}_\ell} \mathbb{E}_{\{\alpha'_\ell\}_{\ell'=1}^{N_S}} \left\{ \frac{|\mathbf{w}_\ell^H \tilde{\mathbf{H}}_\ell \mathbf{g}_{\ell,\text{geo}}|^2}{\sum_{i \neq \ell} |\mathbf{w}_\ell^H \tilde{\mathbf{H}}_i \mathbf{g}_{i,\text{geo}}|^2 + \sigma_n^2 \mathbf{w}_\ell^H \mathbf{w}_\ell} \right\}. \quad (25)$$

A solution to this optimization problem is stated next.

Proposition 2. A linear equalizer \mathbf{w}_ℓ that maximizes the effective mean SINR of the approximated channel $\tilde{\mathbf{H}}$, i.e., a solution to (25), is

$$\mathbf{w}_{\ell,\text{geo}} = \left(\sum_i^{N_S} \sigma_{\alpha_i}^2 \mathbf{a}_i \mathbf{a}_i^H + \bar{\sigma}_n^2 \mathbf{I}_{N_r} \right)^{-1} \mathbf{a}_\ell = (\mathbf{A} \Sigma_{|\alpha|^2} \mathbf{A}^H + \bar{\sigma}_n^2 \mathbf{I}_{N_r})^{-1} \mathbf{a}_\ell \quad (26)$$

where $\bar{\sigma}_n^2 = \frac{\sigma_n^2}{N_t \rho}$ is the inverse signal-to-noise ratio (SNR) and $\Sigma_{|\alpha|^2} = \text{diag}(\sigma_{\alpha_1}^2, \dots, \sigma_{\alpha_{N_S}}^2)$.

Proof: The objective function of (25) is equivalent to

$$\mathbb{E}_{\{\alpha_\ell\}_{\ell'=1}^{N_S}} \{\Gamma_\ell\} |_{\mathbf{H}=\tilde{\mathbf{H}}} = \mathbb{E}_{\{\alpha_\ell\}_{\ell'=1}^{N_S}} \left\{ \frac{N_t \rho |\alpha_\ell \mathbf{w}_\ell^H \mathbf{a}_\ell|^2}{\sum_{i \neq \ell} N_t \rho |\alpha_i \mathbf{w}_\ell^H \mathbf{a}_i|^2 + \sigma_n^2 \mathbf{w}_\ell^H \mathbf{w}_\ell} \right\} \quad (27a)$$

$$= \frac{\mathbb{E}_{\alpha_\ell} \{|\alpha_\ell|^2\} |\mathbf{w}_\ell^H \mathbf{a}_\ell|^2}{\sum_{i \neq \ell} \mathbb{E}_{\alpha_i} \{|\alpha_i|^2\} |\mathbf{w}_\ell^H \mathbf{a}_i|^2 + \frac{\sigma_n^2}{N_t \rho} \mathbf{w}_\ell^H \mathbf{w}_\ell} \quad (27b)$$

$$= \frac{\sigma_{\alpha_\ell}^2 \mathbf{w}_\ell^H \mathbf{a}_\ell \mathbf{a}_\ell^H \mathbf{w}_\ell}{\mathbf{w}_\ell^H \left(\sum_{i \neq \ell} \sigma_{\alpha_i}^2 \mathbf{a}_i \mathbf{a}_i^H + \bar{\sigma}_n^2 \mathbf{I}_{N_r} \right) \mathbf{w}_\ell}. \quad (27c)$$

Observe that this is a generalized Rayleigh quotient. By virtue of Lemma 1 in Appendix A, (27c) is maximized if \mathbf{w}_ℓ is an eigenvector corresponding to the maximum eigenvalue of $\left(\sum_{i \neq \ell} \sigma_{\alpha_i}^2 \mathbf{a}_i \mathbf{a}_i^H + \bar{\sigma}_n^2 \mathbf{I}_{N_r} \right)^{-1} \mathbf{a}_\ell \mathbf{a}_\ell^H$. It is established in [43, §3] that (26) is such an eigenvector. ■

Stacking the individual equalizer $\{\mathbf{w}_i\}_{i=1}^{N_S}$ gives the overall equalizer matrix

$$\mathbf{W}_{\text{geo}} = \mathbf{A}^H (\mathbf{A} \Sigma_{|\alpha|^2} \mathbf{A}^H + \bar{\sigma}_n^2 \mathbf{I}_{N_r})^{-1} = (\Sigma_{|\alpha|^2} \mathbf{A}^H \mathbf{A} + \bar{\sigma}_n^2 \mathbf{I}_{N_S})^{-1} \mathbf{A}^H. \quad (28)$$

Note that the proposed closed-form solution only requires the knowledge of the AoAs $\{\theta_i\}_{i=1}^{N_S}$ from all satellites as well as the SNR $N_t \rho / \sigma_n^2$ and the path losses $\{\sigma_{\alpha_i}^2\}_{i=1}^{N_S}$. Further note, that any $\beta \mathbf{w}_{\ell,\text{geo}}$, with $\beta \neq 0$, is a valid solution for (25). Common choices are $\beta = 1$ [17], or $\beta = 1/|\mathbf{w}_{\ell,\text{geo}}^H \mathbf{H}_\ell \mathbf{g}_\ell|$ [33], [35].

IV. IMPERFECT POSITION KNOWLEDGE

So far, perfect knowledge about the angles θ_ℓ^{el} , θ_ℓ^{az} , Θ_ℓ^{el} and Θ_ℓ^{az} for satellite ℓ has been assumed. Obviously, in practical systems, only an estimate of these angles is available. In this section, the proposed precoder and equalizer are extended to be less sensitive against such estimation errors.

Usually, the AoDs and AoAs are estimated by measuring the phase difference between the antennas, i.e., by estimating the space angles $\phi_\ell^x, \phi_\ell^y, \Phi_\ell^x, \Phi_\ell^y$ first [15], [16]. Due to phase noise, this can only be estimated imperfectly and, therefore, the following error model is considered:¹

$$\hat{\phi}_\ell^x = \phi_\ell^x + v_\ell^x, \quad \hat{\phi}_\ell^y = \phi_\ell^y + v_\ell^y \quad (29a)$$

$$\hat{\Phi}_\ell^x = \Phi_\ell^x + \xi_\ell^x, \quad \hat{\Phi}_\ell^y = \Phi_\ell^y + \xi_\ell^y \quad (29b)$$

where $v_\ell^x, v_\ell^y, \xi_\ell^x, \xi_\ell^y$ are zero mean and statistically independent random variables. Furthermore, v_ℓ^x and v_ℓ^y , and ξ_ℓ^x and ξ_ℓ^y are following the same distribution, respectively. It is further assumed that, for each satellite ℓ , these estimation errors follow the same distribution. Correspondingly, one can define the estimated steering vectors $\hat{\mathbf{a}}_\ell$ and $\hat{\mathbf{b}}_\ell$ by substituting the true angle in (8) with the estimated one. Thus, the elements for satellite ℓ are

$$[\hat{\mathbf{a}}_\ell]_m = \hat{a}_{\ell,m} = e^{j\nu(D_{\text{Rx},m}^x \hat{\phi}_\ell^x + D_{\text{Rx},m}^y \hat{\phi}_\ell^y)}, \quad [\hat{\mathbf{b}}_\ell]_n = \hat{b}_{\ell,n} = e^{j\nu(D_{\text{Tx},n}^x \hat{\Phi}_\ell^x + D_{\text{Tx},n}^y \hat{\Phi}_\ell^y)} \quad (30)$$

A common assumption in the literature is that these estimation errors are uniformly distributed [25], [30], [31], [34], [35]. However, in many applications, such estimation errors are better modeled by a Gaussian distribution [29]. Therefore, we derive the precoder and equalizer for arbitrarily distributed estimation errors and show how to determine them for both, uniform and Gaussian distributed cases. For a better understanding, we first show the statistic relation between the space angles and the corresponding steering vectors, which is related to the characteristic function (CF). Following that, we derive the precoder and equalizer, utilizing the compact notation given with the CF. To the best of the authors' knowledge, this approach is novel within the context of analyzing angular estimation errors.

A. Characteristic Function of Estimation Error

From (29), it follows that the true space angles $\phi_\ell^x, \phi_\ell^y, \Phi_\ell^x$ and Φ_ℓ^y are random variable with mean $\hat{\phi}_\ell^x, \hat{\phi}_\ell^y, \hat{\Phi}_\ell^x$ and $\hat{\Phi}_\ell^y$, respectively. The shape of their PDF is determined by the PDF of $v_\ell^x, v_\ell^y, \xi_\ell^x, \xi_\ell^y$, respectively. Let $f_v(v_\ell^x)$ be the PDF of the estimation error v_ℓ^x . Then, its CF $\varphi_v(t)$ is defined as [44]

$$\varphi_v(t) = \mathbb{E}_{v_\ell^x} \{e^{jtv_\ell^x}\} = \int_{-\infty}^{\infty} f_v(v_\ell) e^{jtv_\ell^x} dv_\ell^x. \quad (31)$$

¹Note that, in principle, it is also possible to directly track the AoA of an incoming wave [36]. However, this is computational more complex due to its high non-linearity and not necessary in the considered scenario.

Hence, the expected value of the m th element $a_{\ell,m}$ of the steering vector \mathbf{a}_ℓ can be written as

$$\mathbb{E}_{v_\ell^x, v_\ell^y} \{a_{\ell,m}\} = \mathbb{E}_{v_\ell^x, v_\ell^y} \left\{ e^{j\nu(D_{\text{Rx},m}^x \phi_\ell^x + D_{\text{Rx},m}^y \phi_\ell^y)} \right\} \quad (32a)$$

$$= e^{j\nu(D_{\text{Rx},m}^x \hat{\phi}_\ell^x + D_{\text{Rx},m}^y \hat{\phi}_\ell^y)} \mathbb{E}_{v_\ell^x} \left\{ e^{-j\nu D_{\text{Rx},m}^x v_\ell^x} \right\} \mathbb{E}_{v_\ell^y} \left\{ e^{-j\nu D_{\text{Rx},m}^y v_\ell^y} \right\} \quad (32b)$$

$$= e^{j\nu(D_{\text{Rx},m}^x \hat{\phi}_\ell^x + D_{\text{Rx},m}^y \hat{\phi}_\ell^y)} \varphi_v(\nu D_{\text{Rx},m}^x) \varphi_v(\nu D_{\text{Rx},m}^y) . \quad (32c)$$

Note that the estimated steering vector $\hat{\mathbf{a}}_\ell$ and the expected value of the true steering vector $\mathbb{E}_{v_\ell^x, v_\ell^y} \{\mathbf{a}_\ell\}$ are not the same, i.e., $\hat{\mathbf{a}}_\ell \neq \mathbb{E}_{v_\ell^x, v_\ell^y} \{\mathbf{a}_\ell\}$.

Similarly, the expected value of the n th element of \mathbf{b}_ℓ can be determined as

$$\mathbb{E}_{\xi_\ell^x, \xi_\ell^y} \{b_{\ell,n}\} = e^{j\nu(D_{\text{Tx},n}^x \hat{\phi}_\ell^x + D_{\text{Tx},n}^y \hat{\phi}_\ell^y)} \varphi_\xi(\nu D_{\text{Tx},n}^x) \varphi_\xi(\nu D_{\text{Tx},n}^y) \quad (33)$$

where $\varphi_\xi(\nu D_{\text{Tx},n}^x)$ and $\varphi_\xi(\nu D_{\text{Tx},n}^y)$ are the CFs of ξ_ℓ^x and ξ_ℓ^y evaluated at $\nu D_{\text{Tx},n}^x$ and $\nu D_{\text{Tx},n}^y$, respectively.

In the following, the expected value for $a_{\ell,m}$ in (32) is evaluated for the special cases of uniform and Gaussian distributed estimation errors. The expected value for $b_{\ell,n}$ can be obtained in the same manner and is thus omitted here.

a) Uniform Distribution: Let $v_\ell^x, v_\ell^y \sim \mathcal{U}(-v_{\max}, v_{\max})$ be uniformly distributed in the interval $[-v_{\max}, v_{\max}]$. Then, $\mathbb{E}_{v_\ell^x, v_\ell^y} \{a_{\ell,m}\}$ can be directly evaluated as [30], [34]

$$\mathbb{E}_{v_\ell^x, v_\ell^y} \{a_{\ell,m}\} \Big|_{v_\ell \sim \mathcal{U}} = \int_{\hat{\phi}_\ell^y - v_{\max}}^{\hat{\phi}_\ell^y + v_{\max}} \int_{\hat{\phi}_\ell^x - v_{\max}}^{\hat{\phi}_\ell^x + v_{\max}} \frac{1}{(2v_{\max})^2} e^{j\nu(D_{\text{Rx},m}^x \phi_\ell^x + D_{\text{Rx},m}^y \phi_\ell^y)} d\phi_\ell^x d\phi_\ell^y \quad (34a)$$

$$= \int_{\hat{\phi}_\ell^x - v_{\max}}^{\hat{\phi}_\ell^x + v_{\max}} \frac{1}{2v_{\max}} e^{j\nu D_{\text{Rx},m}^x \phi_\ell^x} d\phi_\ell^x \cdot \int_{\hat{\phi}_\ell^y - v_{\max}}^{\hat{\phi}_\ell^y + v_{\max}} \frac{1}{2v_{\max}} e^{j\nu D_{\text{Rx},m}^y \phi_\ell^y} d\phi_\ell^y \quad (34b)$$

$$= e^{j\nu D_{\text{Rx},m}^x \hat{\phi}_\ell^x} \text{sinc}(\nu D_{\text{Rx},m}^x v_{\max}) \cdot e^{j\nu D_{\text{Rx},m}^y \hat{\phi}_\ell^y} \text{sinc}(\nu D_{\text{Rx},m}^y v_{\max}) \quad (34c)$$

$$= e^{j\nu(D_{\text{Rx},m}^x \hat{\phi}_\ell^x + D_{\text{Rx},m}^y \hat{\phi}_\ell^y)} \varphi_U(\nu D_{\text{Rx},m}^x) \varphi_U(\nu D_{\text{Rx},m}^y) . \quad (34d)$$

Thus, the CF of a uniform distribution is the sinc-function, i.e., $\varphi_U(t) = \text{sinc}(tv_{\max}) = \sin(tv_{\max})/(tv_{\max})$.

b) Gaussian Distribution: The CF of a zero mean Gaussian distributed random variable with variance σ^2 is also a Gaussian function, i.e., $\varphi_G(t) = e^{-\frac{t^2 \sigma^2}{2}}$ [44, Example 8.5]. Thus, if the estimation error has Gaussian distribution, i.e., $v_\ell^x, v_\ell^y \sim \mathcal{N}(0, \sigma_v^2)$, (32) evaluates to

$$\mathbb{E}_{v_\ell^x, v_\ell^y} \{a_{\ell,m}\} \Big|_{v_\ell \sim \mathcal{N}} = e^{j\nu(D_{\text{Rx},m}^x \hat{\phi}_\ell^x + D_{\text{Rx},m}^y \hat{\phi}_\ell^y)} \varphi_G(\nu D_{\text{Rx},m}^x v_{\max}) \varphi_G(\nu D_{\text{Rx},m}^y v_{\max}) \quad (35a)$$

$$= e^{j\nu(D_{\text{Rx},m}^x \hat{\phi}_\ell^x + D_{\text{Rx},m}^y \hat{\phi}_\ell^y)} e^{-\frac{(\nu D_{\text{Rx},m}^x \sigma_v)^2}{2}} e^{-\frac{(\nu D_{\text{Rx},m}^y \sigma_v)^2}{2}} . \quad (35b)$$

In the following, the CF is used to derive the autocorrelation matrices of the steering vectors, which are necessary for optimum precoder and equalizer design.

B. Precoder

As in Section III-B, the robust precoder \mathbf{G}_{rob} is also designed to maximize the average received power, i.e.,

$$\mathbf{G}_{\text{rob}} \in \arg \max_{\forall \ell: \text{tr}\{\mathbf{G}_\ell^H \mathbf{G}_\ell\} \leq \rho} \mathbb{E}_{\{\alpha_\ell, \xi_\ell^x, \xi_\ell^y\}_{\ell=1}^{N_S}} \left\{ \text{tr} \left\{ \mathbf{G}^H \tilde{\mathbf{H}}^H \tilde{\mathbf{H}} \mathbf{G} \right\} \right\} \quad (36)$$

However, the expected value is now also taken w.r.t. the estimation errors. Thus, the objective function in (36) evaluates to

$$\mathbb{E}_{\{\alpha_\ell, \xi_\ell^x, \xi_\ell^y\}_{\ell=1}^{N_S}} \left\{ \text{tr} \left\{ \mathbf{G}^H \tilde{\mathbf{H}}^H \tilde{\mathbf{H}} \mathbf{G} \right\} \right\} = N_r \text{tr} \left\{ \mathbb{E}_{\{\xi_\ell^x, \xi_\ell^y\}_{\ell=1}^{N_S}} \left\{ \mathbf{G}^H \mathbf{B} \Sigma_{|\alpha|^2} \mathbf{B}^H \mathbf{G} \right\} \right\} \quad (37a)$$

$$= N_r \text{tr} \left\{ \sum_{\ell=1}^{N_S} \sigma_{\alpha_\ell}^2 \mathbb{E}_{\xi_\ell^x, \xi_\ell^y} \left\{ \mathbf{G}_\ell^H \mathbf{b}_\ell \mathbf{b}_\ell^H \mathbf{G}_\ell \right\} \right\} \quad (37b)$$

$$= N_r \sum_{\ell=1}^{N_S} \sigma_{\alpha_\ell}^2 \text{tr} \left\{ \mathbf{G}_\ell^H \mathbf{R}_{\mathbf{b}_\ell} \mathbf{G}_\ell \right\} \quad (37c)$$

where $\mathbf{R}_{\mathbf{b}_\ell} = \mathbb{E}_{\xi_\ell^x, \xi_\ell^y} \left\{ \mathbf{b}_\ell \mathbf{b}_\ell^H \right\}$ is the autocorrelation matrix of the steering vector \mathbf{b}_ℓ . With the CF of the estimation error $\varphi_\xi(t)$ from Section IV-A, the (m, n) th element of the autocorrelation matrix $[\mathbf{R}_{\mathbf{b}_\ell}]_{m,n}$ can be written as (see, e.g., (33))

$$[\mathbf{R}_{\mathbf{b}_\ell}]_{m,n} = \mathbb{E}_{\xi_\ell^x, \xi_\ell^y} \left\{ e^{-j\nu (D_{\text{Tx},m}^{\text{x},\ell} \Phi_\ell^{\text{x}} + D_{\text{Tx},m}^{\text{y},\ell} \Phi_\ell^{\text{y}} - D_{\text{Tx},n}^{\text{x},\ell} \Phi_\ell^{\text{x}} - D_{\text{Tx},n}^{\text{y},\ell} \Phi_\ell^{\text{y}})} \right\} \quad (38a)$$

$$= e^{-j\nu ((D_{\text{Tx},m}^{\text{x}} - D_{\text{Tx},n}^{\text{x}}) \hat{\Phi}_\ell^{\text{x}} + (D_{\text{Tx},m}^{\text{y}} - D_{\text{Tx},n}^{\text{y}}) \hat{\Phi}_\ell^{\text{y}})} \cdot \varphi_\xi(\nu (D_{\text{Tx},m}^{\text{x}} - D_{\text{Tx},n}^{\text{x}})) \varphi_\xi(\nu (D_{\text{Tx},m}^{\text{y}} - D_{\text{Tx},n}^{\text{y}})) \quad (38b)$$

For the special cases of uniform or Gaussian distributed estimation error ξ_ℓ , the elements of $\mathbf{R}_{\mathbf{b}_\ell}$ can be determined in the same way as in (34) or (35). Now, we can formulate the robust precoder, as in the following proposition.

Proposition 3. *Let $\mathbf{g}_{\ell,\text{rob}}$ be a scaled eigenvector corresponding to the largest eigenvalue of $\mathbf{R}_{\mathbf{b}_\ell}$, such that $\mathbf{g}_{\ell,\text{rob}}^H \mathbf{g}_{\ell,\text{rob}} = \rho$, for each satellite ℓ . Then an optimal precoder for (36) is obtained.*

Proof sketch: The sum in (37c) is maximized if each term is maximized independently. Thus, the optimization problem (36) is equivalent to

$$\forall \ell : \min_{\mathbf{G}_\ell} -\text{tr} \left\{ \mathbf{G}_\ell^H \mathbf{R}_{\mathbf{b}_\ell} \mathbf{G}_\ell \right\} \quad \text{s.t.} \quad \text{tr} \left\{ \mathbf{G}_\ell^H \mathbf{G}_\ell \right\} \leq \rho. \quad (39)$$

Following the same steps as for Proposition 1, the optimum precoder \mathbf{G}'_ℓ must satisfy $\mathbf{R}_{\mathbf{b}_\ell} \mathbf{G}'_\ell = \omega'_\ell \mathbf{G}'_\ell$. Consider ω'_ℓ to be the maximum eigenvalue of $\mathbf{R}_{\mathbf{b}_\ell}$. Then, this is satisfied by the proposed precoder $\mathbf{G}_{\ell,\text{rob}} = [\mathbf{0}_{N_t \times (\ell-1)}, \mathbf{g}_{\ell,\text{rob}}, \mathbf{0}_{N_t \times (N_S - \ell)}]$ and the optimum of (39) is achieved, i.e.,

$$-\text{tr} \{ \mathbf{G}_{\ell,\text{rob}}^H \mathbf{R}_{\mathbf{b}_\ell} \mathbf{G}_{\ell,\text{rob}} \} = -\omega'_\ell \mathbf{g}_{\ell,\text{rob}}^H \mathbf{g}_{\ell,\text{rob}} = -\omega'_\ell \rho. \quad (40)$$

■

In Fig. 3, the radiation pattern is shown for three possible precoding approaches with imperfect CSI at the transmitter (CSIT). For the sake of better visibility, only the error in x-direction is considered and $\phi_\ell^y = 0$, and consequently, $\Theta_\ell^{\text{az}} = 0$, is perfectly known. Furthermore, the satellite ℓ is equipped with a uniform linear array (ULA) of $N_t = 60$ antennas, deployed along the local x-axis. The blue line shows the pattern if the power is radiated into the direction of the estimated AoD $\hat{\Theta}_\ell^{\text{el}} = 90^\circ$, i.e., $\mathbf{g}_\ell = \hat{\mathbf{b}}_\ell$. Following the terminology of [26], this approach is called the heuristic approach because the estimation error is not considered at all and the estimated angle is assumed to be the true one. The orange line shows the radiation pattern, if the precoding vector is chosen to be the expected value of the steering vector, i.e., $\mathbf{g}_\ell = \mathbb{E}_{\xi_\ell^x} \{ \mathbf{b}_\ell \}$, and the green line shows the radiation pattern for the optimum precoder, i.e., $\mathbf{g}_\ell = \mathbf{g}_{\ell,\text{rob}}$. Fig. 3a shows the radiation pattern under the assumption of uniform phase errors with $\xi_\ell^x \sim \mathcal{U}(-0.05, 0.05)$ and Fig. 3b for a Gaussian distributed error $\xi_\ell^x \sim \mathcal{N}(0, (2 \cdot 0.05)^2/12)$. Thus, the variance of the estimation error is in both cases the same. It can be observed that the heuristic approach, i.e., the blue lines, leads to the most narrow radiation pattern with the highest peak gain. The second approach gives a much broader main lobe, at the cost of a lower peak gain. Furthermore, a lot of power is transmitted into regions unlikely to contain the GS. With the proposed robust precoder, which is represented by the green line, the main lobe is a little broader than for the heuristic approach. However, the side lobes are further reduced. This becomes clearly visible for the case of uniform estimation error, i.e., the left picture. A phase error of $\xi_{\text{max}} = 0.05$ at $\hat{\Theta}_\ell^{\text{el}} = 90^\circ$ corresponds to an angular error $\hat{\Theta}_\ell^{\text{el}} - \Theta_\ell^{\text{el}} \approx 2.866^\circ$. For the orange line, there is almost constant receive power at the GS over the possible angular region. However, the true AoD must be $87.134^\circ \leq \Theta_\ell^{\text{el}} \leq 92.866^\circ$. Thus, radiating outside this region is a waste of energy and may even cause interference to other systems. Given the proposed robust precoder, only a small amount of the total power is radiated towards $\Theta_\ell^{\text{el}} \leq 87.134^\circ$ and $\Theta_\ell^{\text{el}} \geq 92.866^\circ$. For the Gaussian case, the probability that the true angle is in the interval $[87.134^\circ, 92.866^\circ]$ is

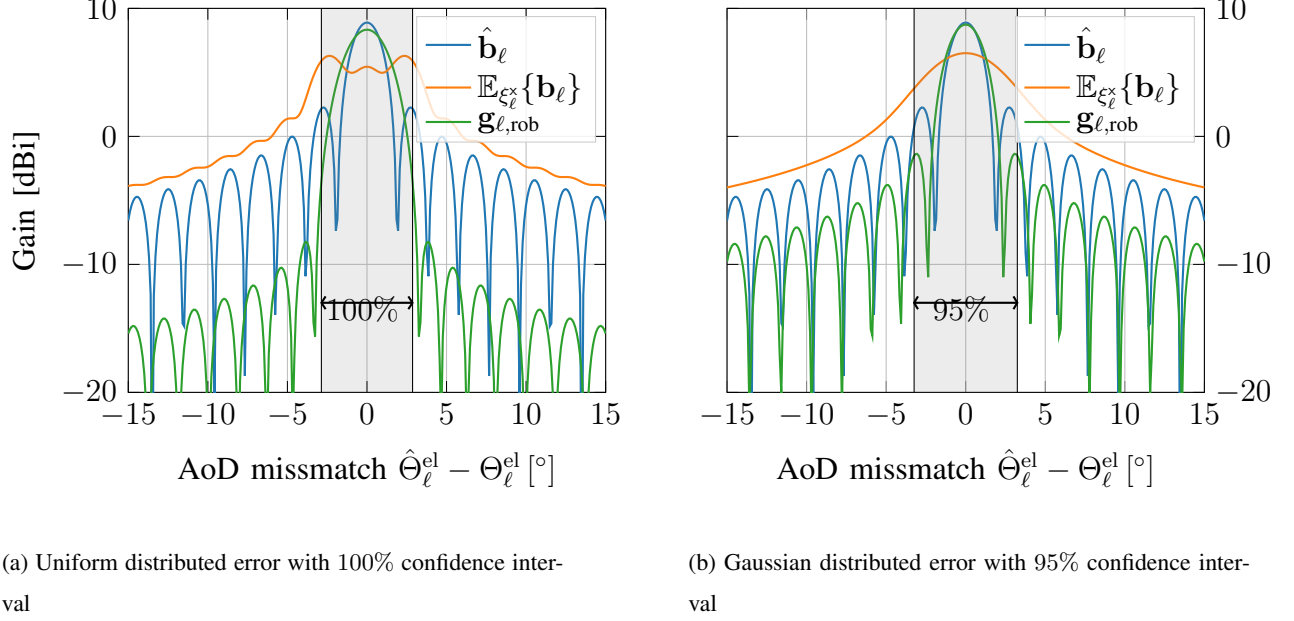


Fig. 3: Radiation pattern for three different precoder $\mathbf{g}_\ell \in \{\hat{\mathbf{b}}_\ell, \mathbb{E}_{\xi_\ell^x} \{\mathbf{b}_\ell\}, \mathbf{g}_{\ell, \text{rob}}\}$ and estimated AoD $\hat{\Theta}_\ell = 90^\circ$.

approximately $\Pr \{87.134^\circ \leq \Theta_\ell^{\text{el}} \leq 92.866^\circ\} |_{v_\ell \sim \mathcal{N}} \approx 92\%$ and the sidelobes are less reduced compared to the uniform case.

C. Equalizer

In this section, the linear equalizer that maximizes the mean SINR with respect to the error model in (29) is derived. Starting from (9) and under the assumption that the geometry based precoder with perfect AoD knowledge (11) is used, the received signal in (1) becomes

$$\mathbf{y} \approx \sum_{\ell=1}^{N_S} \tilde{\mathbf{H}}_\ell \mathbf{g}_{\ell, \text{geo}} s_\ell + \mathbf{n} = \sum_{\ell=1}^{N_S} \alpha_\ell \sqrt{N_t \rho} \mathbf{a}_\ell s_\ell + \mathbf{n}. \quad (41)$$

Then, the optimization problem to determine the robust equalizer becomes

$$\mathbf{w}_{\ell, \text{rob}} \in \arg \max_{\mathbf{w}_\ell} \mathbb{E}_{\{\alpha_{\ell'}, v_{\ell'}^x, v_{\ell'}^y\}_{\ell'=1}^{N_S}} \left\{ \frac{|\mathbf{w}_\ell^H \tilde{\mathbf{H}}_\ell \mathbf{g}_{\ell, \text{geo}}|^2}{\sum_{i \neq \ell} |\mathbf{w}_\ell^H \tilde{\mathbf{H}}_i \mathbf{g}_{i, \text{geo}}|^2 + \sigma_n^2 \mathbf{w}_\ell^H \mathbf{w}_\ell} \right\} \quad (42a)$$

$$= \arg \max_{\mathbf{w}_\ell} \frac{\sigma_{\alpha_\ell}^2 \mathbf{w}_\ell^H \mathbb{E}_{\xi_\ell^x, \xi_\ell^y} \{\mathbf{a}_\ell \mathbf{a}_\ell^H\} \mathbf{w}_\ell}{\mathbf{w}_\ell^H \left(\sum_{i \neq \ell} \sigma_{\alpha_i}^2 \mathbb{E}_{\xi_i^x, \xi_i^y} \{\mathbf{a}_i \mathbf{a}_i^H\} + \bar{\sigma}_n^2 \mathbf{I}_{N_r} \right) \mathbf{w}_\ell} \quad (42b)$$

$$= \arg \max_{\mathbf{w}_\ell} \frac{\sigma_{\alpha_\ell}^2 \mathbf{w}_\ell^H \mathbf{R}_{\mathbf{a}_\ell} \mathbf{w}_\ell}{\mathbf{w}_\ell^H \left(\sum_{i \neq \ell} \sigma_{\alpha_i}^2 \mathbf{R}_{\mathbf{a}_i} + \bar{\sigma}_n^2 \mathbf{I}_{N_r} \right) \mathbf{w}_\ell}. \quad (42c)$$

where $\mathbf{R}_{\mathbf{a}_\ell} = \mathbb{E}_{\xi_\ell^x, \xi_\ell^y} \{\mathbf{a}_\ell \mathbf{a}_\ell^H\}$ is the autocorrelation of the steering vector \mathbf{a}_ℓ . Similiar to (38a), $\mathbf{R}_{\mathbf{a}_\ell}$ is also a Toeplitz matrix and its (m, n) th element is given by

$$\begin{aligned} [\mathbf{R}_{\mathbf{a}_\ell}]_{m,n} &= e^{j\nu((D_{\text{Rx},m}^x - D_{\text{Rx},n}^x)\hat{\phi}_\ell^x + (D_{\text{Rx},m}^y - D_{\text{Rx},n}^y)\hat{\phi}_\ell^y)} \\ &\quad \cdot \varphi_v(\nu(D_{\text{Rx},m}^x - D_{\text{Rx},n}^x)) \varphi_v(\nu(D_{\text{Rx},m}^y - D_{\text{Rx},n}^y)). \end{aligned} \quad (43)$$

The proposed equalizer is stated in the following proposition.

Proposition 4. *The receive vector for satellite ℓ that maximizes the mean SINR is proportional to the eigenvector corresponding to the largest eigenvalue of $\left(\sum_{i \neq \ell} \sigma_{\alpha_i}^2 \mathbf{R}_{\mathbf{a}_i} + \bar{\sigma}_n^2 \mathbf{I}_{N_r}\right)^{-1} \mathbf{R}_{\mathbf{a}_\ell}$.*

Proof sketch: This proof follows along the lines of that of Proposition 2. The objective function in (42) is again a generalized Rayleigh quotient. According to Lemma 1 in Appendix A, it is maximized by the generalized eigenvector corresponding to the largest eigenvalue. ■

In contrast to the case with perfectly known position, no closed form solution for the precoder and equalizer could be found. Instead, it requires the numerical computation of eigenvectors. This leads to slightly higher computational complexity compared to the previous case. Furthermore, it should be noted that only in case of perfect CSI at the receiver (CSIR), the achievable rate is maximized by maximizing the SINR for each satellite [38]. However, for imperfect CSIR, there is no analytic expression for the achievable rate known, which makes it difficult to optimize the equalizer w.r.t. the achievable rate [26].

V. OPTIMAL INTER-SATELLITE DISTANCE

In this section, an analytical solution for the optimal inter-satellite distance is derived. To keep the analysis tractable, we make a few simplifying assumptions. In particular, we assume that the azimuth angles θ_ℓ^{az} , for all satellites ℓ , is zero and that the satellite swarm is flying in a trail formation with constant inter-satellite spacing D_S . This implies that the satellites follow a common orbit with altitude d_0 and the GS's antenna array is effectively seen as a linear array in the orbital plane. We further assume that the GS's antennas are uniformly spaced with distance D_{Rx} . Hence, without loss of generality (given these assumptions), we model the GS's antenna array as a ULA with N_r^x antennas, and the xz-plane of the GS-centered coordinate frame is chosen such that it is aligned with the orbital plane. Besides the GS-centered coordinate frame, we also require an Earth-centered inertial (ECI) coordinate frame whose xz-plane is aligned with the orbital plane. With the Earth's radius being $r_E = 6371$ km, the orbital radius is $r_0 = r_E + d_0$

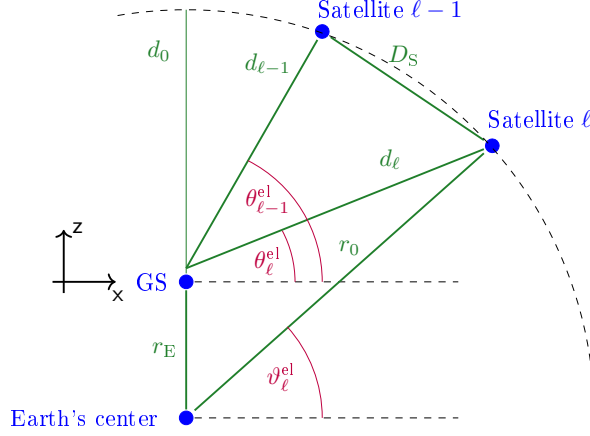


Fig. 4: Geometric relation between two Satellites, ℓ and $\ell - 1$, and the GS for $\theta_\ell^{az} = \theta_{\ell-1}^{az} = 0$.

and the position of satellite ℓ in the ECI coordinate frame is given by the triplet $(r_0, \vartheta_\ell^{\text{el}}, 0)$. Consequently, the GS is located at position $(r_E, \pi/2, 0)$. This setup is illustrated in Fig. 4.

Considering the triangle between satellite ℓ , the GS and the Earth's center as illustrated in Fig. 4, we obtain from the law of sines

$$\vartheta_\ell^{\text{el}} = \theta_\ell^{\text{el}} + \arcsin\left(\frac{r_E}{r_0} \cos(\theta_\ell^{\text{el}})\right) \quad (44)$$

$$d_\ell = r_0 \frac{\cos(\vartheta_\ell^{\text{el}})}{\cos(\theta_\ell^{\text{el}})}. \quad (45)$$

Then, the inter-satellite distance D_S is obtained from the law of cosines as

$$D_S = \sqrt{d_\ell^2 + d_{\ell-1}^2 - 2d_\ell d_{\ell-1} \cos(\theta_{\ell-1}^{\text{el}} - \theta_\ell^{\text{el}})} \quad (46)$$

where $\vartheta_{\ell-1}^{\text{el}}$ and $d_{\ell-1}$ are given analogously to (44) and (45), respectively.

Now, the relation between the inter-satellite distance D_S and the achievable rate is analyzed based on the channel approximation (9). We further approximate the channel gains of all satellites to be equal, i.e., $\sigma_{\alpha_\ell}^2 \approx \sigma_\alpha^2$, for all ℓ . This approximation is valid for small inter-satellite distances but might be not entirely accurate for very large distances. Assuming the precoder \mathbf{G}_{geo} from (11) is employed at the satellites and we have perfect CSIR, the ergodic rate \tilde{R} for $\tilde{\mathbf{H}}$ can be upper bounded as

$$\tilde{R} \leq \log_2 \left| \mathbf{I}_{N_r} + \frac{1}{\sigma_n^2} \mathbb{E}_{\{\alpha_\ell\}_{\ell=1}^{N_S}} \left\{ \tilde{\mathbf{H}} \mathbf{G}_{\text{geo}} \mathbf{G}_{\text{geo}}^H \tilde{\mathbf{H}}^H \right\} \right| = \log_2 \left| \mathbf{I}_{N_r} + \frac{\sigma_\alpha^2}{\sigma_n^2} \mathbf{A} \mathbf{A}^H \right|. \quad (47)$$

Thus, the achievable rate over the channel $\tilde{\mathbf{H}}$ depends on the matrix \mathbf{A} , which is composed of the steering vectors $\{\mathbf{a}_\ell\}_{\ell=1}^{N_S}$.

Due to the trail formation, the swarm is fully described by two parameters: The inter-satellite distance D_S and the number of satellites N_S . Choosing a proper inter-satellite distance D_S is crucial, as it directly impacts the angular spread of the elevation angles between the satellites, which can be used to tune the matrix \mathbf{A} such that the achievable rate is maximized. Therefore, we aim to find an inter-satellite distance $D_{S,\text{opt}}$ such that

$$D_{S,\text{opt}} \in \arg \max_{D_S} \log_2 \left| \mathbf{I}_{N_r} + \frac{\sigma_\alpha^2}{\bar{\sigma}_n^2} \mathbf{A} \mathbf{A}^H \right|. \quad (48)$$

Solving this optimization problem is difficult due to the lack of a clear functional relationship between \mathbf{A} and D_S . A sufficient optimality condition that partially characterizes the solution space of (48) is stated next.

Proposition 5. *Let k be a positive integer such that it is no multiple of N_r^\times . If the elevation angles satisfy*

$$\forall \ell : \forall i \neq \ell : |\cos(\theta_\ell^{\text{el}}) - \cos(\theta_i^{\text{el}})| = \frac{2\pi k}{\nu D_{\text{Rx}} N_r^\times}, \quad (49)$$

then (47) is maximized.

Proof: Observe that (47) is equivalent to

$$\tilde{R} \leq \log_2 \left| \mathbf{I}_{N_S} + \frac{\sigma_\alpha^2}{\bar{\sigma}_n^2} \mathbf{A}^H \mathbf{A} \right| = \log_2 \left(\prod_{\ell=1}^{N_S} \left(1 + \frac{\tilde{\lambda}_\ell \sigma_\alpha^2}{\bar{\sigma}_n^2} \right) \right) \quad (50)$$

where $\tilde{\lambda}_\ell$ are the positive eigenvalues of $\mathbf{A}^H \mathbf{A}$ [37]. Keeping the trace of $\mathbf{A}^H \mathbf{A}$ constant, this is maximized if all eigenvalues have the same value [45, Thm. 2.21]. In other words, any $N_S \times N_S$ matrix $\mathbf{Z} = \mathbf{A}^H \mathbf{A}$ maximizing (50) has a single eigenvalue $\tilde{\lambda}$ with multiplicity N_S .

Further, observe that \mathbf{Z} is a normal matrix. By [42, Thm. 2.5.4], \mathbf{Z} is similar to a diagonal matrix, i.e., there exists a nonsingular matrix \mathbf{S} such that $\mathbf{S}^{-1} \mathbf{A} \mathbf{S} = \mathbf{Z}$ with $\mathbf{\Lambda}$ diagonal. Since similar matrices have the same eigenvalues [42, Cor. 1.3.4], $\mathbf{\Lambda}$ must be $\tilde{\lambda} \mathbf{I}$. Then, for every nonsingular \mathbf{S} , we have $\mathbf{Z} = \mathbf{S}^{-1} \tilde{\lambda} \mathbf{I} \mathbf{S} = \tilde{\lambda} \mathbf{S}^{-1} \mathbf{S} = \tilde{\lambda} \mathbf{I}$. It follows that $\mathbf{Z} = \tilde{\lambda} \mathbf{I}$ is the unique maximizer of (50). For $\mathbf{A}^H \mathbf{A}$ to become a scaled identity matrix, its columns must satisfy $\mathbf{a}_i^H \mathbf{a}_i = \tilde{\lambda}$ and $\mathbf{a}_i^H \mathbf{a}_\ell = 0$ for all i and $\ell \neq i$. From the definition of \mathbf{a} , we obtain

$$\mathbf{a}_i^H \mathbf{a}_\ell = \sum_{m=0}^{N_r-1} e^{j\nu D_{\text{Rx}} m (\cos(\theta_\ell^{\text{el}}) - \cos(\theta_i^{\text{el}}))}. \quad (51)$$

This equals zero if $\nu D_{\text{Rx}} m (\cos(\theta_\ell^{\text{el}}) - \cos(\theta_i^{\text{el}})) = 2\pi \frac{km}{N_r^x}$ for some integer k such that $k \neq nN_r^x$ for all integer n [16]. This is equivalent to the condition above. Finally, observe that

$$\mathbf{a}_i^H \mathbf{a}_i = \sum_{m=0}^{N_r-1} e^{j\nu D_{\text{Rx}} m (\cos(\theta_i^{\text{el}}) - \cos(\theta_i^{\text{el}}))} = \sum_{m=0}^{N_r-1} e^{j0} = N_r^x. \quad (52)$$

■

Consider now two neighbouring satellites ℓ and $\ell - 1$. According to Proposition 5, the first maximum is achieved if

$$\frac{2\pi}{\nu D_{\text{Rx}} N_r^x} = |\cos(\theta_\ell^{\text{el}}) - \cos(\theta_{\ell-1}^{\text{el}})| \Leftrightarrow \quad (53a)$$

$$\theta_{\ell-1} = \begin{cases} \arccos\left(\cos(\theta_\ell^{\text{el}}) - \frac{2\pi}{\nu D_{\text{Rx}} N_r^x}\right) & \text{for } \cos(\theta_\ell^{\text{el}}) \geq \cos(\theta_{\ell-1}^{\text{el}}) \\ \arccos\left(\frac{2\pi}{\nu D_{\text{Rx}} N_r^x} - \cos(\theta_\ell^{\text{el}})\right) & \text{for } \cos(\theta_{\ell-1}^{\text{el}}) \geq \cos(\theta_\ell^{\text{el}}) \end{cases}. \quad (53b)$$

Then, plugging (53b) in (44) and then in (45) and (46), respectively, one gets a solution for the optimal inter-satellite distance $D_{\text{S,opt}}$, which depends on the altitude d_0 , the elevation angle θ_ℓ^{el} of satellite ℓ , the number of receive antennas N_r^x and the antenna spacing D_{Rx} at the GS, as well as the wavenumber ν . As there is little intuition to be gained from the explicit formula for $D_{\text{S,opt}}$ (66), it is delegated to Appendix B.

In Fig. 5, the dependency between the optimum inter-satellite distance $D_{\text{S,opt}}$, the elevation angle θ_ℓ^{el} and number of receive antennas N_r^x is shown for an altitude $d_0 = 600$ km and $\nu D_{\text{Rx}} = \pi$. Note that, according to (49), the product $\nu D_{\text{Rx}} N_r^x$ determines the spatial resolution. Therefore, increasing the antenna spacing D_{Rx} by a certain factor and decreasing the number of antennas N_r^x by the same factor, gives the same results. However, a smaller number of antennas leads to a smaller array gain and if the antenna spacing D_{Rx} and the inter-satellite distance D_{S} are both very large, spatial aliasing must be considered.

It can be seen in Fig. 5 that the optimum inter-satellite distance $D_{\text{S,opt}}$ increases strongly as the elevation angle θ_ℓ^{el} decreases. However, the satellites have distinct elevation angles, i.e., $\theta_\ell^{\text{el}} \neq \theta_i^{\text{el}}$ for all $i \neq \ell$. This means that the optimal distance between satellites i and $i - 1$ is different to the optimal distance between satellite ℓ and $\ell - 1$. Furthermore, the elevation angles changes over time. Thus, it is not possible to ensure orthogonal steering vectors between all satellites, i.e., $\mathbf{a}_i^H \mathbf{a}_\ell = 0$ for all $i \neq \ell$, during the whole flight with a constant inter-satellite distance D_{S} . Adjusting the inter-satellite distance during the flight, however, requires additional fuel and increased complexity for flight control and should thus be avoided. Nevertheless, as

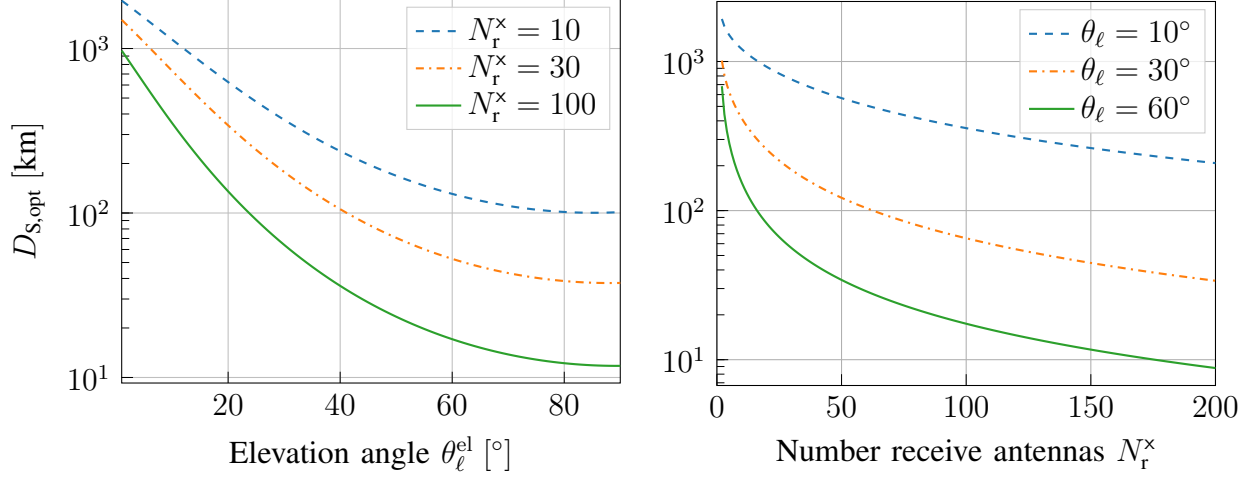


Fig. 5: Optimal inter-satellite distances $D_{S,\text{opt}}$ for different elevation angles θ_ℓ^{el} and for different number of receive antennas N_r^x at altitude $d_0 = 600$ km.

evaluated numerically in Section VI, the channel capacity is not decreasing much after the first local optimum and, thus, a close-to-optimal heuristic is obtained by relaxing condition (49). In particular, the average rate over the whole flight is close to maximum if

$$\min_{\ell} |\cos(\theta_\ell^{\text{el}}) - \cos(\theta_{\ell-1}^{\text{el}})| \geq \frac{2\pi}{\nu D_{\text{Rx}} N_r^x} \quad (54)$$

holds during the transmission. This can be used as a guidance to find a proper inter-satellite distance D_S , if the minimum elevation angle is known a priori.

Furthermore, the following relation between the optimal inter-satellite distance and the optimal precoder can be observed.

Proposition 6. *The proposed precoder in (11) is capacity achieving for the channel $\tilde{\mathbf{H}}$ if $|\cos(\theta_\ell^{\text{el}}) - \cos(\theta_i^{\text{el}})| = \frac{2\pi k}{\nu D_{\text{Rx}} N_r^x}$ for all $\ell \neq i$ and $|\alpha_i| = |\alpha_\ell| = |\alpha|$.*

Proof: First, recall from the proof of Proposition 1 that the channel $\tilde{\mathbf{H}}$ can be decomposed as $\tilde{\mathbf{H}} = \mathbf{A}\Sigma_\alpha\mathbf{B}^H$. Second, the capacity achieving precoder is given by the scaled dominant right singular vectors of the channel matrix [37]. The SVD of the channel $\tilde{\mathbf{H}}$ is defined as $\tilde{\mathbf{H}} = \tilde{\mathbf{U}}\tilde{\Sigma}\tilde{\mathbf{V}}^H$, where $\tilde{\mathbf{U}}$ and $\tilde{\mathbf{V}}$ are unitary matrices and $\tilde{\Sigma}$ is a diagonal matrix with non-negative numbers on its main diagonal.

The complex-valued diagonal matrix Σ_α is equivalent to

$$\Sigma_\alpha = \text{diag}(|\alpha_1|, \dots, |\alpha_{N_S}|) \cdot \text{diag}(e^{-j\phi_1}, \dots, e^{-j\phi_{N_S}}) = \Sigma_{|\alpha|}\Sigma_\phi = \Sigma_\phi\Sigma_{|\alpha|}. \quad (55)$$

Furthermore, due to the block diagonal structure of \mathbf{B} , we have $\mathbf{B}^H \mathbf{B} = N_t \mathbf{I}_{N_S}$ and, if (49) holds, we also have $\mathbf{A}^H \mathbf{A} = N_r^x \mathbf{I}_{N_S}$. Thus, we can define the unitary matrices $\tilde{\mathbf{U}}$ and $\tilde{\mathbf{V}}$ as

$$\tilde{\mathbf{U}} = \frac{1}{\sqrt{N_r^x}} [\mathbf{A}, \tilde{\mathbf{u}}_{N_S+1}, \dots, \tilde{\mathbf{u}}_{N_r^x}] \begin{bmatrix} \boldsymbol{\Sigma}_\phi & \mathbf{0}_{(N_r^x-N_S) \times (N_r^x-N_S)} \\ \mathbf{0}_{(N_r^x-N_S) \times (N_r^x-N_S)} & \mathbf{I}_{N_r^x-N_S} \end{bmatrix} \quad (56a)$$

$$\tilde{\mathbf{V}} = \frac{1}{\sqrt{N_t}} [\mathbf{B}, \tilde{\mathbf{v}}_{N_S+1}, \dots, \tilde{\mathbf{v}}_{N_{Tx}}] \quad (56b)$$

where $[\tilde{\mathbf{u}}_{N_S+1}, \dots, \tilde{\mathbf{u}}_{N_r^x}]$ and $[\tilde{\mathbf{v}}_{N_S+1}, \dots, \tilde{\mathbf{v}}_{N_{Tx}}]$ are the left and right singular vectors belonging to the nullspace of $\tilde{\mathbf{H}}$, respectively. Consequently, the singular values are given by $|\alpha_i|$, i.e.,

$$\tilde{\boldsymbol{\Sigma}} = \sqrt{N_r^x N_t} \begin{bmatrix} \boldsymbol{\Sigma}_{|\alpha|} & \mathbf{0}_{N_S \times (N_{Tx}-N_S)} \\ \mathbf{0}_{(N_r^x-N_S) \times N_S} & \mathbf{0}_{(N_r^x-N_S) \times (N_{Tx}-N_S)} \end{bmatrix}. \quad (57)$$

Consequently, the channel $\tilde{\mathbf{H}}$ can be decomposed as

$$\tilde{\mathbf{H}} = \tilde{\mathbf{U}} \tilde{\boldsymbol{\Sigma}} \tilde{\mathbf{V}}^H = \mathbf{A} \boldsymbol{\Sigma}_\phi \boldsymbol{\Sigma}_{|\alpha|} \mathbf{B} = \sqrt{\frac{N_t}{\rho}} \mathbf{A} \boldsymbol{\Sigma}_\phi \boldsymbol{\Sigma}_{|\alpha|} \mathbf{G}_{\text{geo}}. \quad (58)$$

Thus, the right singular vectors of $\tilde{\mathbf{H}}$ are given by the proposed precoder (11). Furthermore, if $|\alpha_i| = |\alpha_\ell| = |\alpha|$ for all i and ℓ holds, i.e., $\boldsymbol{\Sigma}_{|\alpha|} = |\alpha| \mathbf{I}_{N_S}$, then all precoding vectors $\mathbf{g}_{\ell, \text{geo}}$ must have the same power in order to achieve the capacity. This is given by the proposed precoder, as $\|\mathbf{g}_{\ell, \text{geo}}\|_2^2 = \|\mathbf{g}_{i, \text{geo}}\|_2^2 = \rho$ for all i and ℓ . ■

Note that several simplifying assumptions have been made in this section. Therefore, the precoder and the inter-satellite distance are only optimal for distinct setups. In general they are sub-optimal. However, as shown in Section VI, the numerical simulations show an almost optimal performance under more practical assumptions of the proposed precoder (11) in combination with the linear equalizer (26) at the optimal inter-satellite distance (66), as well. Furthermore, compared to the optimal SVD-based precoder, the requirements on CSI acquisition are considerably relaxed and there is no need for any inter-satellite communication in order to determine the precoder matrix. Moreover, the computational complexity is also significantly reduced.

VI. NUMERICAL EVALUATIONS

A. Channel Model

We use the channel model recommended by 3GPP and ITU-R in [39], [46]–[49]. It is further assumed, that the GS is placed such that the communication link is not blocked by other objects. The carrier frequency is $f_c = 20$ GHz and we assume a pure LOS connection between the GS

and each satellite. With the possibility of non-LOS (NLOS) propagation, swarms with more satellites get a further advantage due to a higher probability that at least one satellite has a LOS connection to the GS. For the sake of fairer comparison, NLOS propagation is not considered. The (m, n) th element of the local channel matrix \mathbf{H}_ℓ is modeled as

$$h_{m,n}^\ell = \frac{1}{\sqrt{L_{m,n}^\ell}} e^{-j(\nu d_{m,n}^\ell + \phi_{\text{atm},\ell})} \quad (59)$$

where $\phi_{\text{atm},\ell} \in [0, 2\pi]$ is a uniformly distributed phase shift caused by the atmosphere, and L is the path loss, which is given in decibel as [39]

$$L_{m,n}^\ell|_{\text{dB}} = 20 \log_{10} (2\nu d_{m,n}) - (\zeta_{\text{Tx,dB}} + \zeta_{\text{Rx,dB}}) + L_{\text{sf},\ell} + L_{\text{cl},\ell} + L_{\text{gas},\ell} + L_{\text{ts},\ell} \quad (60)$$

where $L_{\text{sf},\ell} \sim \mathcal{N}(0, \sigma_{\text{sf},\ell}^2)$ and $L_{\text{cl},\ell}$ are the shadow fading and clutter loss, respectively. In LOS $L_{\text{cl},\ell} = 0$ dB and $\sigma_{\text{sf},\ell}^2$ depends on the AoA. The specific values can be found in [39], while in this paper the rural scenario has been considered. $L_{\text{gas},\ell}$ includes atmospheric gas absorption described in [46] using the reference standard atmosphere [47]. Eventually, $L_{\text{ts},\ell}$ includes the losses due to tropospheric scintillation, as summarized in [48], [49], and $\zeta_{\text{Tx,dB}}$ and $\zeta_{\text{Rx,dB}}$ are the transmit and receive antenna gains, respectively. In all simulations, the transmission is assumed to start if the average elevation angle over all satellites $\theta_{\text{mean}}^{\text{el}} = 1/N_S \sum_{\ell=1}^{N_S} \theta_\ell^{\text{el}} = 30^\circ$, i.e., the evaluation is done for $30^\circ \leq \theta_{\text{mean}}^{\text{el}} \leq 150^\circ$. Furthermore, the noise power and altitude are set to $P_{\text{N,dB}} = -120$ dBW and $d_0 = 600$ km, respectively.

B. Inter-Satellite Distance

In Section V, the optimal inter-satellite distance $D_{\text{S,opt}}$ for a simplified scenario has been derived. In order to verify that derivation, we assume, in this subsection, $\theta_\ell^{\text{az}} = 0$ for all satellites ℓ and a constant inter-satellite distance D_S . As in Section V, we model the GS antenna array as an effective ULA. The number of receive antennas is $N_r^x = 100$ and the receive antenna gain is $\zeta_{\text{Rx,dB}} = 20$ dBi. In practical systems, this antenna gain can be achieved, e.g., with an 100×100 URA. Likewise, we assume a ULA with $N_t^x = 60/N_S$ antennas and an antenna gain of $\zeta_{\text{Tx,dB}} = 17.8$ dBi at each satellite. The sum transmit power of the satellite swarm is $P_{\text{Tx}} = N_S \rho = 10$ W. The normalization of the number of transmit antennas and the transmit power per satellite w.r.t. to the number of satellites N_S is included to allow a fairer comparison between satellite swarms with different N_S . The channel capacity R_{opt} from (4) is considered as a benchmark. It requires SVD precoding and successive interference cancellation (SIC) at the

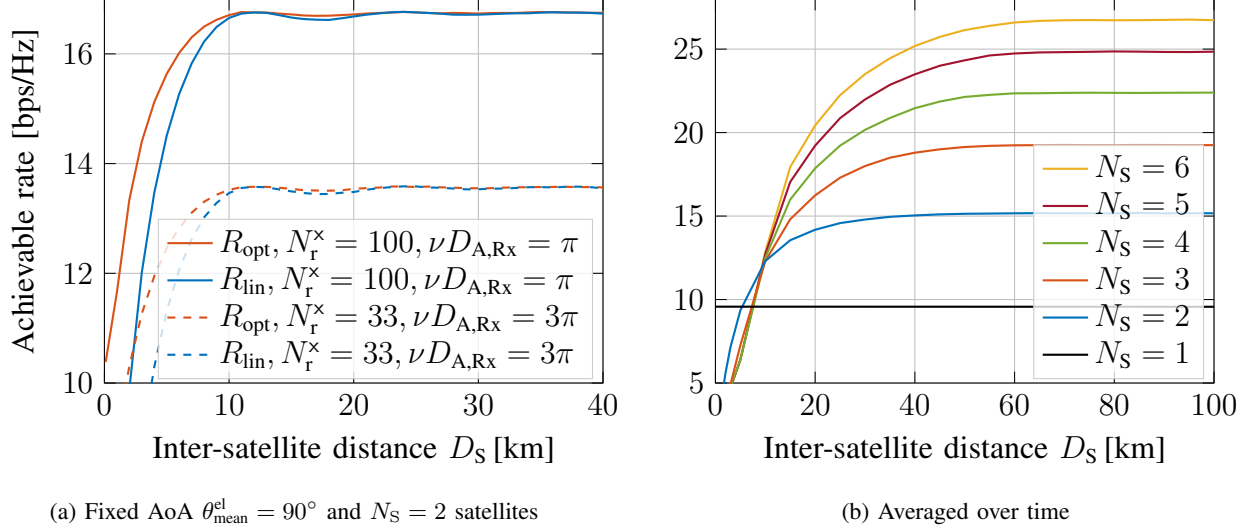


Fig. 6: Achievable rate performance in dependence of different inter-satellite distances D_S with $\theta_\ell^{\text{az}} = 0$ for all ℓ .

GS [37], [38]. This is compared against the geometric precoder (11) with linear equalizer (26). The corresponding achievable rate is given by R_{lin} in (23).

In Fig. 6a, the achievable rate is shown as a function of the inter-satellite distance D_S with a fixed average elevation angle $\theta_{\text{mean}}^{\text{el}} = 90^\circ$. Furthermore, two different antenna arrays at the GS have been assumed in Fig. 6a. The solid lines are for an array with $N_r^x = 100$ receive antennas and an antenna spacing of half of the wavelength, i.e., $\nu D_{Rx} = \pi$, which is also assumed in the rest of this paper. For the dashed lines, the number of receive antennas is $N_r^x = 33$, while the antenna spacing is 1.5 times the carrier wavelength, i.e., $\nu D_{Rx} = 3\pi$. According to the derivation from Section V, the achievable rate must have its maximum every $D_{S,\text{opt}} = 12$ km, for both receive apertures. It can be seen, that this is fulfilled for the channel capacity R_{opt} as well as the achievable rate with our proposed linear transceiver approach R_{lin} . For inter-satellite distances $D_S > 12$ km, the achievable rate oscillates slightly, while every $D_{S,\text{opt}} = 12$ km the maximum is obtained. The overall rate for $N_r^x = 33$ is less than with $N_r^x = 100$ antennas, which is due to the smaller array gain. Considering the proposed precoding and equalization approach, one can observe, that the capacity is achieved at the optimal inter-satellite distances. Additionally, for $D_S > 12$ km, the achievable rate is still close to the optimum. However, for $D_S < 12$ km, the proposed approach leads to a rate reduction compared to optimal transceivers. This is mainly due to the linear equalization and could be alleviated by using SIC at the GS.

In real world applications, the time averaged rate is of greater interest than the rate at a fixed

time instance. Therefore, in Fig. 6b, the achievable rate is averaged over a complete satellites pass. Then, there are no more periodic variations of the achievable rate, but the achievable rate stays constant for $D_S \geq 65$ km. This corresponds to the optimum inter-satellite distance at the minimum elevation angle $\theta_{\text{mean,min}}^{\text{el}} = 30^\circ$ and holds for all considered number of satellites $N_S \in \{2, 3, 4, 5, 6\}$, which justifies the heuristic (54).

C. Imperfect Position Knowledge

Next, the performance of the proposed precoder and equalizer is evaluated under more practical assumptions. We assume $N_S = 2$ satellites with a constant inter-satellite distance $D_S \in \{26 \text{ km}, 52 \text{ km}\}$, each equipped with an 8×8 URA, while the GS has an 16×16 URA. The corresponding antenna gains are $\zeta_{\text{Tx,dB}} = 17.4$ dBi and $\zeta_{\text{Rx,dB}} = 15.6$ dBi, respectively, and the antenna spacing for all arrays is $D_{\text{Tx}} = D_{\text{Rx}} = 6$ cm. In this case, the overall array gains, i.e., $\zeta_{\text{Tx,dB}} + 10 \log_{10}(N_S N_t) = 38.5$ dBi and $\zeta_{\text{Rx,dB}} + 10 \log_{10}(N_r) = 39.7$ dBi, matches with the 3GPP recommendations [50]. The corresponding achievable rates are shown in Fig. 7 w.r.t. the sum transmit power P_{Tx} . In both graphs, uniform estimation errors of the space angles at the satellites and the GS are assumed, i.e., $\xi_\ell^x, \xi_\ell^y \sim \mathcal{U}(-\xi_{\text{max}}, \xi_{\text{max}})$ and $v_\ell^x, v_\ell^y \sim \mathcal{U}(-v_{\text{max}}, v_{\text{max}})$, with $\xi_{\text{max}} = 1/16$ and $v_{\text{max}} \in \{1/16, 1/32\}$. The purple lines show the performance of the proposed robust transceiver from Section IV. The green lines show the performance of a heuristic approach, where the precoder and equalizer are calculated with (11) and (26), respectively, by substituting the true angles with the estimated ones. As benchmark, the channel capacity R_{opt} is included. It can be seen that by including the statistic of the error, the performance degradation due to imperfect position knowledge is reduced. According to previous observations, the optimal inter-satellite for $N_r^x = 16$ and $\nu D_{\text{Rx}} = 8\pi$ should be at $D_{S,\text{opt}} \approx 52$ km. Given that inter-satellite distance, the channel capacity is achieved with the proposed transceiver approach, under perfect position knowledge, i.e., $R_{\text{opt}} \approx R_{\text{lin}}$, for both the heuristic and the robust one. Thus, given the proposed linear precoder and equalizer, the channel capacity can be achieved by transmitting independent data streams, which avoids time-critical inter-satellite communication, and without the necessity of SIC at the GS. Further increasing the inter-satellite distance does not increase the capacity R_{opt} nor the achievable rate R_{lin} . However, as observed in Fig. 7a, even at lower inter-satellite distances the same rate can be achieved. In case of imperfect position knowledge, the performance with a smaller inter-satellite distance decreases stronger than for larger distances.

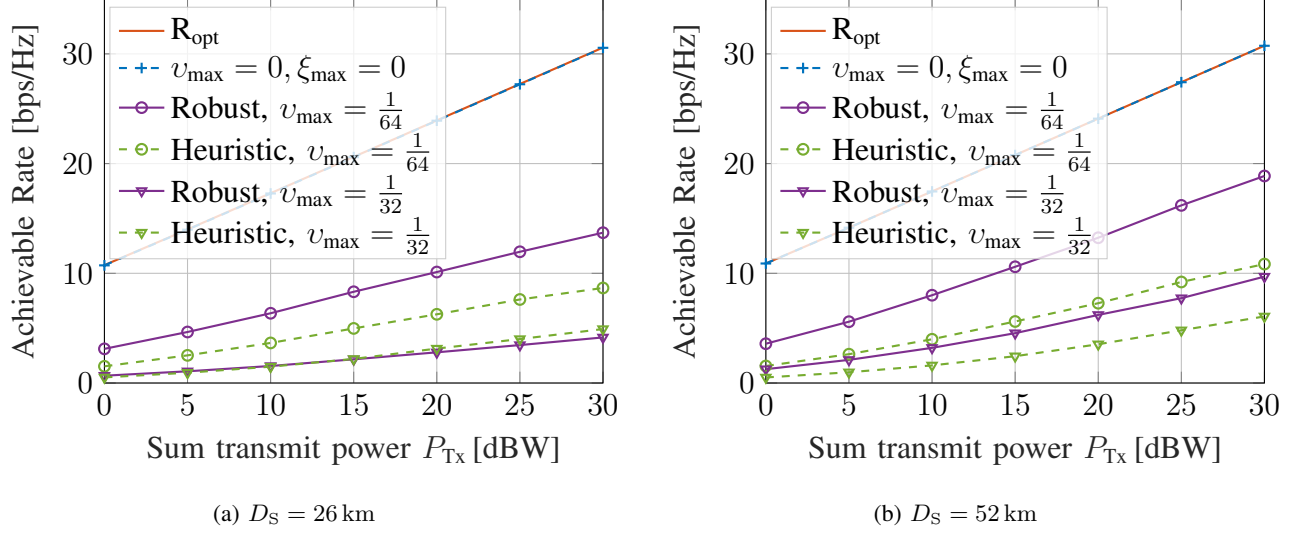


Fig. 7: Achievable rate performance for robust precoder and equalizer.

VII. CONCLUSION

In this paper, a low complexity distributed precoder for satellite swarms and a linear equalizer, both utilizing the geometric relation between the positions of the satellites and GS, has been proposed. Furthermore, the inter-satellite distance has been optimized for a specific scenario. Given that the inter-satellite distances are chosen adequately, it has been shown that the proposed transceiver architecture achieves a performance very close to the capacity upper bound obtained by assuming perfect CSI and instantaneous coordination between satellites. This almost optimal performance is achieved without any inter-satellite communication between the satellites, for the precoder design. Furthermore, the requirements for channel estimation are significantly reduced, as only relative positional knowledge between the satellites and the GS are necessary. If the relative positions are estimated erroneously, knowledge about the statistic of the estimation error can be exploited to reduce the performance degradation. However, not all issues in real world scenarios have been considered in this paper, e.g., finite length channel codes and discrete modulation schemes must be used in practical communications and the LOS connection can be blocked. This effects will lead to an overall performance degradation in over-the-air transmission. Nevertheless, it has been shown that in the downlink, by applying the proposed approaches, the achievable rate can be significantly increased for satellite swarms compared to single satellite systems, while keeping the computational complexity and signaling overhead for precoding and equalization low.

APPENDIX A

GENERALIZED RAYLEIGH QUOTIENT

Lemma 1. Let $\mathbf{A} \in \mathbb{C}^{n \times n}$ be Hermitian and $\mathbf{B} \in \mathbb{C}^{n \times n}$ Hermitian positive definite. Then,

$$\max_{\mathbf{x} \in \mathbb{C}^n \setminus \{\mathbf{0}\}} \frac{\mathbf{x}^H \mathbf{A} \mathbf{x}}{\mathbf{x}^H \mathbf{B} \mathbf{x}} = \lambda_{\max}(\mathbf{A}, \mathbf{B}), \quad (61)$$

where $\lambda_{\max}(\mathbf{A}, \mathbf{B})$ is the maximum generalized eigenvalue. The optimal \mathbf{x} in (61) is an eigenvector corresponding to $\lambda_{\max}(\mathbf{A}, \mathbf{B})$.

Proof: Let $\mathbf{L}\mathbf{L}^H$ be the Cholesky factorization of \mathbf{B} . Substitute $\mathbf{y} = \mathbf{L}^H \mathbf{x}$ in the LHS of (61). Then,

$$\max_{\mathbf{x} \in \mathbb{C}^n \setminus \{\mathbf{0}\}} \frac{\mathbf{x}^H \mathbf{A} \mathbf{x}}{\mathbf{x}^H \mathbf{L}\mathbf{L}^H \mathbf{x}} = \max_{\mathbf{y} \in \mathbb{C}^n \setminus \{\mathbf{0}\}} \frac{\mathbf{y}^H \mathbf{L}^{-1} \mathbf{A} \mathbf{L}^{-H} \mathbf{y}}{\mathbf{y}^H \mathbf{y}} = \lambda_{\max}(\mathbf{L}^{-1} \mathbf{A} \mathbf{L}^{-H}), \quad (62)$$

where the last step is due to the Rayleigh-Ritz Theorem [42, Thm. 4.2.2].

Recall that two square matrices \mathbf{C}, \mathbf{D} are similar if there exists a nonsingular matrix \mathbf{S} such that $\mathbf{D} = \mathbf{S}^{-1} \mathbf{C} \mathbf{S}$. By virtue of [42, Cor. 1.3.4], similar matrices have the same eigenvalues. Since $\mathbf{L}^{-1} \mathbf{A} \mathbf{L}^{-H}$ and $(\mathbf{L}\mathbf{L}^H)^{-1} \mathbf{A}$ are similar with similarity matrix \mathbf{L}^H , $\lambda_{\max}(\mathbf{L}^{-1} \mathbf{A} \mathbf{L}^{-H}) = \lambda_{\max}(\mathbf{B}^{-1} \mathbf{A}) = \lambda_{\max}(\mathbf{A}, \mathbf{B})$.

Let $\tilde{\mathbf{y}}$ be an eigenvector of $\mathbf{L}^{-1} \mathbf{A} \mathbf{L}^{-H}$ corresponding to the maximum eigenvalue λ_{\max} . Then, by [42, Def. 1.1.2], $\mathbf{L}^{-1} \mathbf{A} \mathbf{L}^{-H} \tilde{\mathbf{y}} = \lambda_{\max} \tilde{\mathbf{y}}$. Multiplying both sides from the left by $\tilde{\mathbf{y}}^H$ and substituting $\tilde{\mathbf{y}} = \mathbf{L}^H \tilde{\mathbf{x}}$, we obtain

$$(\mathbf{L}^H \tilde{\mathbf{x}})^H \mathbf{L}^{-1} \mathbf{A} \mathbf{L}^{-H} (\mathbf{L}^H \tilde{\mathbf{x}}) = \lambda_{\max} (\mathbf{L}^H \tilde{\mathbf{x}})^H (\mathbf{L}^H \tilde{\mathbf{x}}) \quad \Leftrightarrow \quad \tilde{\mathbf{x}}^H \mathbf{A} \tilde{\mathbf{x}} = \lambda_{\max} \tilde{\mathbf{x}}^H \mathbf{B} \tilde{\mathbf{x}}. \quad (63)$$

This establishes that $\mathbf{L}^H \tilde{\mathbf{x}}$ maximizes $\mathbf{x}^H \mathbf{A} \mathbf{x} / (\mathbf{x}^H \mathbf{B} \mathbf{x})$. Due to similarity and the fact that $\tilde{\mathbf{y}}$ is an eigenvector of $\mathbf{L}^{-1} \mathbf{A} \mathbf{L}^{-H}$ corresponding to λ_{\max} , $\tilde{\mathbf{x}}$ is an eigenvector of $\mathbf{B}^{-1} \mathbf{A}$ [42, Thm. 1.4.8]. ■

APPENDIX B

EXPLICIT FORMULA FOR $\mathbf{D}_{\text{S,OPT}}$

For the sake of brevity, only the case $\cos(\theta_{\ell}^{\text{el}}) \geq \cos(\theta_{\ell-1}^{\text{el}})$ is considered here. The formula for the other case can be found in the same way. With (53b) and (44), $\vartheta_{\ell-1}^{\text{el}}$ can be written as a function of the elevation angle $\theta_{\ell}^{\text{el}}$ of satellite ℓ and the receive array parameters $\nu D_{\text{Rx}} N_{\text{r}}^{\text{x}}$

$$\vartheta_{\ell-1}^{\text{el}} = \arccos \left(\cos(\theta_{\ell}^{\text{el}}) - \frac{2\pi}{\nu D_{\text{Rx}} N_{\text{r}}^{\text{x}}} \right) + \arcsin \left(\frac{r_{\text{E}}}{r_0} \left(\cos(\theta_{\ell}^{\text{el}}) - \frac{2\pi}{\nu D_{\text{Rx}} N_{\text{r}}^{\text{x}}} \right) \right). \quad (64)$$

Now, with (45), the distances d_ℓ and $d_{\ell-1}$ can be written as a function of θ_ℓ^{el} , the receive array parameters $\nu D_{\text{Rx}} N_{\text{r}}$ as well as the orbital radius r_0

$$d_{\ell-1} = r_0 \frac{\cos \left(\arccos \left(\cos(\theta_\ell^{\text{el}}) - \frac{2\pi}{\nu D_{\text{Rx}} N_{\text{r}}^{\text{x}}} \right) + \arcsin \left(\frac{r_{\text{E}}}{r_0} \left(\cos(\theta_\ell^{\text{el}}) - \frac{2\pi}{\nu D_{\text{Rx}} N_{\text{r}}^{\text{x}}} \right) \right) \right)}{\cos(\theta_\ell^{\text{el}}) - \frac{2\pi}{\nu D_{\text{Rx}} N_{\text{r}}^{\text{x}}}} \quad (65a)$$

$$d_\ell = r_0 \frac{\cos \left(\theta_\ell^{\text{el}} + \arcsin \left(\frac{r_{\text{E}}}{r_0} \cos(\theta_\ell^{\text{el}}) \right) \right)}{\cos(\theta_\ell^{\text{el}})}. \quad (65b)$$

Finally, plugging (65) into (46) gives the smallest optimal inter-satellite distance $D_{\text{S,opt}}$

$$D_{\text{S,opt}} = r_0^2 \left[\left(\frac{\cos \left(\theta_\ell^{\text{el}} + \arcsin \left(\frac{r_{\text{E}}}{r_0} \cos(\theta_\ell^{\text{el}}) \right) \right)}{\cos(\theta_\ell^{\text{el}})} \right)^2 + \left(\frac{\cos \left(\arccos \left(\cos(\theta_\ell^{\text{el}}) - \frac{2\pi}{\nu D_{\text{Rx}} N_{\text{r}}^{\text{x}}} \right) + \arcsin \left(\frac{r_{\text{E}}}{r_0} \left(\cos(\theta_\ell^{\text{el}}) - \frac{2\pi}{\nu D_{\text{Rx}} N_{\text{r}}^{\text{x}}} \right) \right) \right)}{\cos(\theta_\ell^{\text{el}}) - \frac{2\pi}{\nu D_{\text{Rx}} N_{\text{r}}^{\text{x}}}} \right)^2 - 2 \frac{\cos \left(\theta_\ell^{\text{el}} + \arcsin \left(\frac{r_{\text{E}}}{r_0} \cos(\theta_\ell^{\text{el}}) \right) \right)}{\cos(\theta_\ell^{\text{el}})} \cdot \frac{\cos \left(\arccos \left(\cos(\theta_\ell^{\text{el}}) - \frac{2\pi}{\nu D_{\text{Rx}} N_{\text{r}}^{\text{x}}} \right) + \arcsin \left(\frac{r_{\text{E}}}{r_0} \left(\cos(\theta_\ell^{\text{el}}) - \frac{2\pi}{\nu D_{\text{Rx}} N_{\text{r}}^{\text{x}}} \right) \right) \right)}{\cos(\theta_\ell^{\text{el}}) - \frac{2\pi}{\nu D_{\text{Rx}} N_{\text{r}}^{\text{x}}}} \right]^{\frac{1}{2}} \cdot \cos \left(\arccos \left(\cos(\theta_\ell^{\text{el}}) - \frac{2\pi}{\nu D_{\text{Rx}} N_{\text{r}}^{\text{x}}} \right) - \theta_\ell^{\text{el}} \right) \quad (66)$$

REFERENCES

- [1] M. Röper, B. Matthiesen, D. Wübben, P. Popovski, and A. Dekorsy, “Beamspace MIMO for satellite swarms,” in *Proc. IEEE Wireless Commun. Netw. Conf. (WCNC)*, Austin, TX, USA, Apr. 2022.
- [2] 3GPP, “Study on using satellite access in 5G,” *TR 22.822 V16.0.0*, Jun. 2018.
- [3] O. Kodheli *et al.*, “Satellite communications in the new space era: A survey and future challenges,” *IEEE Commun. Surveys Tuts*, vol. 23, no. 1, pp. 70–109, Jan.–Mar. 2021.
- [4] I. del Portillo, B. G. Cameron, and E. F. Crawley, “A technical comparison of three low earth orbit satellite constellation systems to provide global broadband,” *Acta Astronaut.*, vol. 159, pp. 123–135, Jun. 2019.
- [5] B. Di, L. Song, Y. Li, and H. V. Poor, “Ultra-dense LEO: Integration of satellite access networks into 5G and beyond,” *IEEE Trans. Wireless Commun.*, vol. 26, no. 2, pp. 62–69, Apr. 2019.
- [6] I. Leyva-Mayorga, B. Soret, M. Röper, D. Wübben, B. Matthiesen, A. Dekorsy, and P. Popovski, “LEO small-satellite constellations for 5G and beyond-5G communications,” *IEEE Access*, vol. 8, pp. 184 955–184 964, Oct. 2020.
- [7] G. Zheng, S. Chatzinotas, and B. Ottersten, “Generic optimization of linear precoding in multibeam satellite systems,” *IEEE Trans. Wireless Commun.*, vol. 11, no. 6, pp. 4695–4707, Jun. 2012.
- [8] V. Joroughi, M. A. Vazquez, and A. I. Perez-Neira, “Precoding in multigateway multibeam satellite systems,” *IEEE Trans. Wireless Commun.*, vol. 15, no. 7, pp. 4944–4956, Jul. 2016.

- [9] A. I. Perez-Neira, M. A. Vazquez, M. B. Shankar, S. Maleki, and S. Chatzinotas, "Signal processing for high-throughput satellites: Challenges in new interference-limited scenarios," *IEEE Signal Process. Mag.*, vol. 36, no. 4, Jul. 2019.
- [10] C. Verhoeven, M. Bentum, G. Monna, J. Rotteveel, and J. Guo, "On the origin of satellite swarms," *Acta Astronaut.*, vol. 68, no. 7, pp. 1392–1395, Apr.–May 2011.
- [11] R. Radhakrishnan *et al.*, "Survey of inter-satellite communication for small satellite systems: Physical layer to network layer view," *IEEE Commun. Surveys Tuts.*, vol. 18, no. 4, pp. 2442–2473, 4th Quart. 2016.
- [12] G.-P. Liu and S. Zhang, "A survey on formation control of small satellites," *Proc. IEEE*, vol. 106, no. 3, Mar. 2018.
- [13] A. Budianu, A. Meijerink, and M. Bentum, "Swarm-to-Earth communication in OLFAR," *Acta Astronaut.*, vol. 107, pp. 14–19, Feb.–Mar. 2015.
- [14] R. Richter, I. Bergel, Y. Noam, and E. Zehavi, "Downlink cooperative MIMO in LEO satellites," *IEEE Access*, vol. 8, pp. 213 866–213 881, Nov. 2020.
- [15] A. Im, D. Kerr, H. Lu, S. Wu, Z. Aliyazicioglu, and H. K. Hwang, "Angle of arrival estimation using MIMO array antenna," in *Proc. MTS/IEEE OCEANS*, Bergen, Norway, Jun. 2013.
- [16] H. Lin, F. Gao, S. Jin, and G. Y. Li, "A new view of multi-user hybrid massive MIMO: Non-orthogonal angle division multiple access," *IEEE J. Sel. Areas Commun.*, vol. 35, no. 10, pp. 2268–2280, Oct. 2017.
- [17] L. You, K. X. Li, J. Wang, X. Gao, X. G. Xia, and B. Ottersten, "Massive MIMO transmission for LEO satellite communications," *IEEE J. Sel. Areas Commun.*, vol. 38, no. 8, pp. 1851–1865, Aug. 2020.
- [18] R. T. Schwarz, T. Delamotte, K. Storek, and A. Knopp, "MIMO applications for multibeam satellites," *IEEE Trans. Broadcast.*, vol. 65, no. 4, pp. 664–681, Dec. 2019.
- [19] I. Ahmed *et al.*, "A survey on hybrid beamforming techniques in 5G: Architecture and system model perspectives," *IEEE Commun. Surveys Tuts.*, vol. 20, no. 4, pp. 3060–3097, Oct.–Dec. 2018.
- [20] F. Yamashita, K. Kobayashi, M. Ueba, and M. Umehira, "Broadband multiple satellite MIMO system," in *Proc. IEEE Veh. Tech. Conf. (VTC)*, vol. 4, Dallas, TX, USA, Sep. 2005, pp. 2632–2636.
- [21] D. Goto, H. Shibayama, F. Yamashita, and T. Yamazato, "LEO-MIMO satellite systems for high capacity transmission," in *Proc. IEEE Glob. Commun. Conf. (GLOBECOM)*, Abu Dhabi, United Arab Emirates, Dec. 2018.
- [22] K. Liolis, A. Panagopoulos, and P. Cottis, "Multi-satellite MIMO communications at Ku-band and above: Investigations on spatial multiplexing for capacity improvement and selection diversity for interference mitigation," *EURASIP J. Wireless Commun. Netw.*, Dec. 2007.
- [23] M. Röper and A. Dekorsy, "Robust distributed MMSE precoding in satellite constellations for downlink transmission," in *Proc. IEEE 2nd 5G World Forum (5GWF)*, Dresden, Germany, Sep.–Oct. 2019, pp. 642–647.
- [24] W. Guo, A.-A. Lu, X. Gao, and X.-G. Xia, "Broad coverage precoder design for synchronization in satellite massive MIMO systems," *IEEE Trans. Commun.*, vol. 69, no. 8, pp. 5531–5545, Aug. 2021.
- [25] Z. Lin, M. Lin, B. Champagne, W. Zhu, and N. Al-Dhahir, "Robust hybrid beamforming for satellite-terrestrial integrated networks," in *Proc. IEEE Int. Conf. Acoustics, Speech and Signal Process. (ICASSP)*, Barcelona, Spain, May 2020.
- [26] F. Dietrich, *Robust Signal Processing for Wireless Communications*, ser. Foundations in Signal Processing, Communications and Networking. Springer-Verlag Berlin Heidelberg, 2008.
- [27] A. Abrardo, G. Fodor, M. Moretti, and M. Telek, "MMSE receiver design and SINR calculation in MU-MIMO systems with imperfect CSI," *IEEE Wireless Commun. Lett.*, vol. 8, no. 1, pp. 269–272, Feb. 2019.
- [28] Y. Guo and B. Levy, "Robust MSE equalizer design for MIMO communication systems in the presence of model uncertainties," *IEEE Trans. Signal Process.*, vol. 54, no. 5, pp. 1840–1852, May 2006.
- [29] D. Mi, M. Dianati, L. Zhang, S. Muhaidat, and R. Tafazolli, "Massive MIMO performance with imperfect channel reciprocity and channel estimation error," *IEEE Trans. Commun.*, vol. 65, no. 9, pp. 3734–3749, Sep. 2017.

- [30] S. Bazzi and W. Xu, "Robust Bayesian Precoding for Mitigation of TDD Hardware Calibration Errors," *IEEE Signal Process. Lett.*, vol. 23, no. 7, pp. 929–933, Jul. 2016.
- [31] L. Sun *et al.*, "A robust secure hybrid analog and digital receive beamforming scheme for efficient interference reduction," *IEEE Access*, vol. 7, pp. 22 227–22 234, Feb. 2019.
- [32] B. Carlson, "Covariance matrix estimation errors and diagonal loading in adaptive arrays," *IEEE Trans. Aerosp. Electron. Syst.*, vol. 24, no. 4, pp. 397–401, Jul. 1988.
- [33] K. Bell, Y. Ephraim, and H. Van Trees, "A bayesian approach to robust adaptive beamforming," *IEEE Trans. Signal Process.*, vol. 48, no. 2, pp. 386–398, Feb. 2000.
- [34] X. Mao, W. Li, Y. Li, Y. Sun, and Z. Zhai, "Robust adaptive beamforming against signal steering vector mismatch and jammer motion," *International Journal of Antennas and Propagation*, pp. 247–267, Jul. 2015.
- [35] Z. Li, Y. Zhang, Q. Ge, and B. Xue, "A robust deceptive jamming suppression method based on covariance matrix reconstruction with frequency diverse array MIMO radar," in *Proc. IEEE Int. Conf. on Signal Process., Commun. Comput. (ICSPCC)*, Xiamen, China, Oct. 2017.
- [36] J. Zhao, F. Gao, W. Jia, S. Zhang, S. Jin, and H. Lin, "Angle domain hybrid precoding and channel tracking for millimeter wave massive MIMO systems," *IEEE Trans. Wireless Commun.*, vol. 16, no. 10, pp. 6868–6880, Oct. 2017.
- [37] E. Telatar, "Capacity of multi-antenna gaussian channels," *Eur. Trans. Telecommun.*, vol. 10, no. 6, Nov.–Dec. 1999.
- [38] D. Tse and P. Viswanath, *Fundamentals of Wireless Communication*. Cambridge, U.K.: Cambridge Univ. Press, 2005.
- [39] 3GPP, "Study on new radio (NR) to support non-terrestrial networks," *TR 38.811 V15.2.0*, Sep. 2019.
- [40] K. Storek, C. A. Hofmann, and A. Knopp, "Measurements of phase fluctuations for reliable MIMO space communications," in *Proc. IEEE Asia-Pac. Conf. Wireless Mob. (APWiMob)*, Bandung, Indonesia, Aug. 2015, pp. 157–162.
- [41] D. P. Bertsekas, *Nonlinear Programming*, 2nd ed., ser. Athena scientific optimization and computation series. Belmont (Mass.): Athena Scientific, 1999.
- [42] R. A. Horn and C. R. Johnson, *Matrix Analysis*. Cambridge, U.K.: Cambridge Univ. Press, 1990.
- [43] P. Patcharamaneepakorn, S. Armour, and A. Doufexi, "On the equivalence between SLNR and MMSE precoding schemes with single-antenna receivers," *IEEE Commun. Lett.*, vol. 16, no. 7, pp. 1034–1037, Jul. 2012.
- [44] H. Kobayashi, B. L. Mark, and W. Turin, *Probability, Random Processes, and Statistical Analysis: Applications to Communications, Signal Processing, Queueing Theory and Mathematical Finance*. Cambridge University Press, 2011.
- [45] E. A. Jorswieck and H. Boche, *Majorization and Matrix Monotone Functions in Wireless Communications*, ser. FnT Commun. Inf. Theory. Boston, MA, USA: Now, 2007, vol. 3, no. 6.
- [46] ITU-R, "Attenuation by atmospheric gases and related effects," *ITU-R P.676-12*, Aug. 2019.
- [47] —, "Reference standard atmospheres," *ITU-R P.835-6*, Dec. 2017.
- [48] —, "Propagation data and prediction method required for the design of Earth-space telecommunication systems," *ITU-R P.618-13*, Dec. 2017.
- [49] —, "Ionospheric propagation data and prediction methods required for the design of satellite networks and systems," *ITU-R P.531-14*, Aug. 2019.
- [50] 3GPP, "Solutions for NR to support non-terrestrial networks (NTN)," *TR 38.821 V16.0.0*, Dec. 2019.